

12-5-2017

Surface Enhanced Raman Scattering (SERS) Substrates and Probes

Srismrita Basu

Louisiana State University and Agricultural and Mechanical College, sbasu9@lsu.edu

Follow this and additional works at: https://digitalcommons.lsu.edu/gradschool_dissertations



Part of the [Electrical and Computer Engineering Commons](#)

Recommended Citation

Basu, Srismrita, "Surface Enhanced Raman Scattering (SERS) Substrates and Probes" (2017). *LSU Doctoral Dissertations*. 4177.
https://digitalcommons.lsu.edu/gradschool_dissertations/4177

This Dissertation is brought to you for free and open access by the Graduate School at LSU Digital Commons. It has been accepted for inclusion in LSU Doctoral Dissertations by an authorized graduate school editor of LSU Digital Commons. For more information, please contact gradetd@lsu.edu.

SURFACE ENHANCED RAMAN SCATTERING (SERS) SUBSTRATES AND PROBES

A Dissertation

Submitted to the Graduate Faculty of the
Louisiana State University and
Agricultural and Mechanical College
in partial fulfillment of the
requirements for the degree of
Doctor of Philosophy

in

Division of Electrical and Computer Engineering
The School of Electrical Engineering and Computer Science

by

Srismrita Basu

B.Sc, University of Calcutta, India 2006

M.Sc, University of Calcutta, India 2008

M.Tech, West Bengal University of Technology, India 2010

May 2018

Dedicated to

Srikumar Bose

Debisree Bose

Subhodip Maulik

& Those who helped me in my hard times

ACKNOWLEDGEMENTS

The majority of this research was performed in the Electronic Material Device Laboratory (EMDL), at Electrical and Computer Engineering Department. Some of the work was performed in Center for Advanced Microstructures and Devices (CAMD), Louisiana State University (LSU).

I would like to express my profound gratitude to all of those who believed in me throughout my research work. First of all, I would like to thank deeply my advisor Dr. Martin Feldman (Marty). This work would not have been possible without his constant support, patience, encouragement, and belief of me from the very first day at LSU. I will never forget his caring nature and extremely understanding attitude towards his students. He is possibly the most intelligent person I have met in my life. His ideas and way of working with simple things simply amazed me, and I would like to follow his path of living and working throughout my life. He is a true leader, and I am honored that I am his student.

I feel truly privileged to have Dr. Theda Daniels-Race, Dr. Ashok Srivastava, Dr. Lavonda Brown, and Dr. Tammy Dugas on in my committee. I have been associated with Dr. Race and Dr. Srivastava from the day I joined LSU. I took 4 courses from Dr. Srivastava, and he is amazing. Not only as a teacher but as a human being he is so supportive and caring. Dr. Race's unflinching support and guidance means a lot to me. Her way of thinking and expert advice as a successful woman motivated me throughout my Ph.D. work. I am really touched by the polite and helpful nature of Dr. Brown, which made me comfortable during my interactions with her.

I would like to extend my gratitude to Dr. Mandi Lopez and Dr. Michael Mathis, for providing the biological samples from their laboratories. Their valuable suggestions helped me to work with biological tissues, and obtained the results.

I am thankful to the department of Division of Electrical and Computer Engineering (ECE) and department of Continuing Education for the financial support. I would like to mention that I am very much grateful to ECE department for choosing me for 4 consecutive years for the prestigious Jayanti and Suresh Rai scholarship.

I would like to thank Mr. Christopher E O' Loughlin for being not just a lab manager but being a friend who is always there for me to rely upon in research endeavors. I acknowledge the contribution of my colleagues/ friends Dr. Hsaun Chao Hou, Dr. Jeonghwan Kim, for all their help and advice.

Above all I am really grateful to my parents, Baba (Srikumar Bose) and Maa (Debisree Bose) for their infinite love. This was their dream and without them, I would not have been anywhere in my life.

I would like to thank my in laws (Sumitra Maulik and Pradip kumar Maulik) for their support, and encouragement, Chiranjeev Chatterjee (Nawab da) for always being there with me when I was down, and making me positive. I would like to thank Shre Chatterjee (Shre da) for motivating me since we met.

Last but not the least; I would also like to thank Subhodip Maulik (my husband). I would never have come to USA for a PhD, and survive if you were not in my life. So, this is yours as well.

TABLE OF CONTENTS

ACKNOWLEDGEMENTS.....	iii
LIST OF TABLES.....	vii
LIST OF FIGURES.....	viii
ABSTRACT.....	xii
CHAPTER 1. BRIEF DESCRIPTION OF CHAPTER CONTENT	1
CHAPTER 2. INTRODUCTION.....	3
2.1. Raman Scattering.....	3
2.2. Raman Spectrometer.....	8
2.3. Surface Enhanced Raman Scattering (SERS)	10
2.4. Materials Used For Surface Enhanced Raman Scattering (SERS)	11
CHAPTER 3. MOTIVATION AND RESEARCH GOALS	13
CHAPTER 4. NANO COST SURFACE ENHANCED RAMAN SCATTERING (SERS) SUBSTRATE USING ALUMINUM FOIL AND GOLD.....	15
4.1. Introduction	15
4.2. Raman Methods.....	15
4.3. Specimen Preparation.....	16
4.4. Substrate Preparation.....	18
4.5. Conclusions.....	27
CHAPTER 5. SINGLE FIBER BASED SURFACE ENHANCED RAMAN SCATTERING (SERS) PROBE DESIGN.....	28
5.1. Introduction	28
5.2. Theory:.....	29
5.3. Experimental	34
5.4. Connecting Probe at the End of the Articulate Arm	38
5.5. Conclusions	41
CHAPTER 6. DETECTION USING THE PROBE SET UP.....	42
6.1. Introduction	42
6.2. Detection of Gelatin Using Different Concentrations of Rhodamine 6G Solutions.....	42
6.3. Detection of Various Mouse Tissues.....	45
6.4. Detection of Cancerous Tumor of a Mouse	47
6.5. Conclusions	50
CHAPTER 7. SURFACE ENHANCED RAMAN SPECTROSCOPIC SUBSTRATE UTILIZING GOLD NANOPARTICLES ON CARBON NANOTUBES.....	52
7.1. Introduction.....	52

7.2. Experimental Procedure.....	54
7.3. Results.....	57
7.4. Conclusion.....	64
CHAPTER 8. SURFACE ENHANCED RAMAN SPECTROSCOPIC SUBSTRATE USING GOLD NANO-PARTICLES ON THINNED SILICON WAFER.....	66
8.1. Introduction.....	66
8.2. Substrate Preparation.....	67
8.3. Results.....	71
8.4. Conclusion.....	75
CHAPTER 9. SUMMARY AND RECOMMENDATIONS FOR FUTURE WORK.....	76
9.1. Summary of Results.....	76
9.2. Recommendations for future work.....	77
9.3. Final Remarks.....	78
REFERENCES.....	79
APPENDIX A: PERMISSION TO REPRINT FROM REVIEW OF SCIENTIFIC INSTRUMENTS	87
APPENDIX B: PERMISSION TO REPRINT FROM JOURNAL OF VACUUM SCIENCE B, NANOTECHNOLOGY & MICROELECTRONICS : MATERIALS, PROCESSING, MEASUREMENT, AND PHENOMENA.....	90
APPENDIX C: PERMISSION TO REPRINT FROM JOURNAL OF APPLIED PHYSICS.....	93
VITA.....	95

LIST OF TABLES

Table 2.1 Plasmon resonance wavelengths for gold, silver, copper, and aluminum.....	12
Table 4.1 Raman intensities of 1mM R6G solution on different types of aluminum foil without gold on both the front and the back side	19
Table 4.2 Raman intensities of 1mM R6G solution for different etching times to determine the optimum etching time for enhancement	21
Table 4.3 Raman intensities of 1mM R6G solution on different types of aluminum foil with gold on both the front and the back side	23
Table 5.1 Raman intensities for different microscope objectives and Probe with different numerical apertures	30
Table 6.1 Raman intensities for gelatin prepared by different concentrations of R6G solutions measured by needle probe connected with the articulate arm to the Raman spectrometer.....	44
Table 6.2 Ratios of the intensities of Raman spectral lines, ν_1 to ν_2 , for cancerous tumors and healthy mouse colon cells. In all four cases, the ratios are much larger for tumors than for healthy colons, with differences of many standard deviations.....	50
Table 7.1 Raman intensities of 1mM R6G solution for different types of substrates (CNT layer on back side of etched-stirred aluminum foil).....	59
Table 7.2 Signals from a 1mm suspension of R6G on different substrates.....	65
Table 8.1 Specification of the Silicon wafer.....	66
Table 8.2 Comparison of different type of epoxies.....	68
Table 8.3 Specifications of the set up.....	69
Table 9.1 Comparison of 3 newly developed SERS substrates.....	76

LIST OF FIGURES

Figure 2.1 The first Raman spectrometer, built by C.V. Raman.....	3
Figure 2.2 Incident light scattered in different directions.....	4
Figure 2.3 Rayleigh and Raman scattering.....	6
Figure 2.4 Schematic diagram of a Raman spectrometer.....	9
Figure 2.5 LABRAM Raman specrometer at EMDL in LSU.....	9
Figure 4.1 In Vitro/ Conventional method of SERS.....	15
Figure 4.2 <i>Ex Vivo</i> SERS Probe	16
Figure 4.3 Chemical structure of Rhodamine 6G.....	17
Figure 4.4 Different concentrations of R6G solutions for <i>in vitro</i> measurements.....	17
Figure 4.5 Gelatin prepared with different concentrations of R6G solutions varying from 1nM to 1mM for <i>ex vivo</i> like measurements.....	18
Figure 4.6 (a) Photograph of the Aluminum foil (98.5% - 99.9% pure aluminum), (b) Photograph of the Aluminum pellets (99.9999% pure aluminum).....	20
Figure 4.7 (a) Raman spectrum of the non-etched Aluminum foil, (b) Raman spectrum of the non -etched Aluminum pellet.....	20
Figure 4.8: Schematic diagram of the DC powered magnetron sputtering machine.....	22
Figure 4.9 SEM image of sputtered gold on back side of the stirring etched aluminum foil.....	24
Figure 4.10 Process of obtaining Raman signal using <i>ex vivo</i> like method.....	25
Figure 4.11 Raman spectrum of DI water and R6G solutions (concentration varies from 1nM to 1mM by a factor of 10) using <i>ex vivo</i> like method. Over a factor of one million, the Raman signal changed by a factor of 10.....	26
Figure 4.12 Raman signals (using 50x microscope objective) for viewing on gold as a function of the concentration of R6G solutions.....	27
Figure 5.1 (a) Long single fiber system, (b) Two fiber system.....	29

Figure 5.2 Surface Enhanced Raman signal strength as a function of numerical aperture. Except for point “F”, all the data were taken through microscope objectives focused on the same rough metallic sample. F was taken through an optical fiber, and the data has been compensated for a 50% insertion loss. The straight line is a fit to Raman intensity proportional to the square of the numerical aperture.....30

Figure 5.3 Surface enhanced Raman scattering signal strength as a function of focus for a 50X, NA= 0.55 microscope objective. A gaussian fit is shown for comparison. The FWHN is roughly 9 μm , much larger than the nominal depth of focus of the objective.....31

Figure 5.4 A two fiber SERS system. Single mode laser light exits the top fiber interacts with nano particles in the shaded region, and generated Raman light which enters the bottom fiber in the zero order.....32

Figure 5.5 (a) SEM image of 20 nm of sputtered gold on aluminum foil. (b) SEM image of 20 nm of gold after epoxying to glass and etching away the aluminum. The characteristic closely packed gold globules form an ideal surface for enhancing Raman scattering.....34

Figure 5.6 Schematic diagram of the GRIN lens coupled fiber.....35

Figure 5.7 (a) Simplified sketch, not to scale, of GRIN lens and optical fiber assembly. For clarity, the fiber jacket, etc., have been omitted (b) Stainless steel needle epoxyed in place (c) Gold covered foil epoxyed under pressure to the fiber (d) Aluminum dissolved in etch, leaving a thin layer of gold epoxyed to the fiber (e) Photograph of the finished probe.....36

Figure 5.8 (a) Side view of the fiber before etching under 20X microscope objective, and (b) side view of the fiber after etching under 20x microscope objective.....37

Figure 5.9 Wooden structure with spring used for applying pressure to thin the epoxy at the end of the fiber..... 38

Figure 5.10 Schematic diagram of the articulate arm connected to probe and Raman spectrometer..... 39

Figure 5.11 Photograph of the whole system.....40

Figure 5.12 Raman spectrum obtained from needle in air and DI water. The red spectrum is from the needle probe in air and the blue spectrum is from needle probe in DI water..... 42

Figure 6.1 Photograph of the probe at the end of articulate arm inserted in Gelatin block.....43

Figure 6.2 Raman spectrum of Gelatin made with 1mM R6G solution using the needle probe connected with the articulate arm.....43

Figure 6.3 Intensity vs. R6G concentration in gelatin.....45

Figure 6.4 Raman spectra for (a) Lungs, (b) Kidney, (c) Heart, (d) Liver, (e) Skin, and (f) Muscle from freshly removed organs of mice using the needle probe connected with the Raman spectrometer through the articulate arm.....	46
Figure 6.5 Photograph of (a) needle probe in healthy colon, (b) healthy colon taken out from a freshly sacrificed mouse.....	47
Figure 6.6 Photograph of (a) needle probe in cancerous tumor, (b) cancerous tumor taken out from a freshly sacrificed mouse	48
Figure 6.7 Raman spectra obtained by a needle probe into mouse colon. The dotted curve is for a healthy colon, the solid curve is for a cancerous colon tumor.....	48
Figure 7.1 (a) Single walled carbon nanotube (SWCNT), (b) Multi walled carbon nanotube (MWCNT) (Triple layer).....	53
Figure 7.2: Drop casting method. Gold was sputtered after the MWCNT were deposited.....	56
Figure 7.3 (a) SEM image of CNT deposited on stirred-etched aluminum foil (b) SEM image of 20nm sputtered gold on CNT deposited on stirred-etched aluminum foil. Both the images were taken with 100,000 X magnification.....	57
Figure 7.4 <i>In vitro</i> arrangement for SERS.....	58
Figure 7.5 Raman signal (with a microscope objective of NA=0.55) 1mM R6G solution on gold covered MWCNT on etched-stirred Aluminum foil.....	59
Figure 7.6 Raman signals of R6G solutions (using 50x microscope objective) for gold on MWCNT on the back side of etched-stirred Aluminum foil as a function of the wave number, Concentration of R6G vary from 1nM to 1mM by a factor of 10.....	60
Figure 7.7 Process of sample preparation and measurement for <i>ex vivo</i> like method.....	61
Figure 7.8 Raman signals of R6G solutions (using microscope objective of NA= 0.55) for viewing through gold on the back side of etched-stirred Aluminum foil, after ashed the MWCNT layer, as a function of the wavenumber, Concentration of R6G vary from 1nM to 1mM by a factor of 10.	62
Figure 7.9 Raman signals (using 50x microscope objective) for viewing through epoxy and gold after ashing as a function of the concentration of R6G solutions (Red solid curve), and Raman signals (using 50x microscope objective) for gold on MWCNT on the back side of etched-stirred Aluminum foil as a function of the concentration of R6G solutions (Blue dotted curve).....	63
Figure 7.10 Raman signal of 1mM R6G solution in gelatin using optical fiber probe developed Au coated MWCNT on Al foil.....	64

Figure 8.1 Photograph of the <1-0-0> Silicon wafer.....	66
Figure 8.2 (a) Photograph of the set up for etching using small tube (b) Photograph of the set up for etching using large tube.....	70
Figure 8.3 Optical image of the Silicon wafer after removing 120 μ m using small tube to define the etched area	70
Figure 8.4 SEM image of the sputtered Au on smooth side of the silicon wafer under 30.0K magnification.....	71
Figure 8.5 Raman spectrum of the 1mM R6G solution on the SERS substrate and on the smooth side of the bare Si wafer was obtained. The blue curve is the spectrum from 1mM R6G solution on the gold SERS substrate, and the red curve is the spectrum from 1mM R6G solution on the smooth side of the bare Si wafer.....	72
Figure 8.6 Raman signals of R6G solutions (using microscope objective of NA= 0.55) for viewing on gold on the smooth side of silicon wafer, as a function of the wave number, Concentration of R6G vary from 1nM to 1mM by a factor of 10.....	73
Figure 8.7 Raman signals (using 50x microscope objective) for viewing on gold as a function of the concentration of R6G solutions.....	74
Figure 8.8 Raman signal of 1mM R6G in gelatin using optical fiber probe developed Au coated silicon wafer.....	75

ABSTRACT

Raman spectroscopy is a well-known technique for complex molecular detection. In Raman spectrometry, laser beam is focused on a sample to generate a unique "fingerprint" of the molecule. The Raman signal is very weak. To overcome this problem nano rough metallic substrates are fabricated to enhance the signal strength. In clinical applications, remote contact and minimally invasive probes inside the specimen are needed.

This research work is divided in: (1) development of Surface Enhanced Raman Scattering (SERS) substrate using gold coated etched aluminum foil, (2) development of the SERS probe using the aluminum based substrate with a single optical fiber and GRIN lens connected to the Raman spectrometer by an articulate arm, (3) differentiation of the cancerous and benign colon of a mouse, (4) development of a SERS substrate using gold-coated Multi-wall Carbon Nanotube (MWCNT) on etched aluminum, and (5) development of another SERS substrate using gold-coated etched silicon wafer.

A low cost clinical probe is developed by using an optical fiber, a gradient-index (GRIN) lens, and a SERS substrate for molecular imaging to detect biological specimens. A low-cost SERS substrate is fabricated from aluminum foil covered with 20nm of gold. The optical fiber connected to a GRIN lens is inside a 0.5mm diameter stainless steel needle. The nano-rough metallic substrate is glued to the end of the fiber by a thin layer of epoxy. Different concentrations of gelatins and various biological tissues have been detected by this probe connected with a 1m long air path in an articulate arm. Previous work manufactured probes with long single fiber and two short fibers. This needle probe successfully overcomes the problems

associated with them. The observed Raman signal is comparable to the signal produced by a microscope objective of the same numerical aperture.

To obtain a highly sensitive SERS substrate, a rough nano-metallic structure is developed by sputtering gold nano particles on the MWCNT laden etched aluminum foil. Another SERS substrate is fabricated by depositing gold nano particles on the smooth side of the silicon wafer after thinning it down from 420 μm to 120 μm for the development of clinical probes in future.

CHAPTER 1: BRIEF DESCRIPTION OF CHAPTER CONTENT

This chapter gives a brief description of the chapters 2 to 9 of this work.

Chapter 2 (“Introduction”) first gives a brief description of Raman Scattering and Raman Spectrometer. It describes the working principle of Raman scattering and the advantages and disadvantages. Then it includes the requirements of Surface Enhanced Raman Scattering (SERS) and specifically why gold is the metal chosen for this research.

Chapter 3 (“Motivation and Research Goals”) explains the motivation of the work and the goals to which this research is directed. The motivation behind the development of a 0.5mm diameter probe using a single optical fiber is stated.

Chapter 4 (“Nano Cost Surface Enhanced Raman Scattering (SERS) Substrate Using Aluminum Foil and Gold”) describes the fabrication process of a SERS substrate using Aluminum foil with a thin layer of sputtered gold on it. Experimental data is given to detect the required parameters for this SERS substrate fabrication. In addition, the *in vitro*/ conventional method and the *ex vivo*/ probe method are compared along with proper specimen preparation for the enhancement measurement purpose.

Chapter 5 (“Single Fiber Surface Enhanced Raman Scattering (SERS) Probe Design”) describes a unique method of designing a single optical fiber based thin needle probe. It also shows how remote measurement of the sample is possible using this probe connected with a previously prepared 1-meter long air path in an articulate arm. The advantages of this single fiber system are explained there.

Chapter 6 (“Detection Using the Probe Set up”) discusses the detection of Rhodium 6G with a gelatin specimen, prepared with different concentrations of Rhodamine 6G solution. A brief description of cancer detection in mouse tissue is given as well along with the detection of

various tissues of a mouse. The chapter concludes with the advantage of using this system in place of biopsies for cancer detection.

Chapter 7 (“Surface Enhanced Raman Spectroscopic Substrate Utilizing Gold Nanoparticles on Carbon Nanotubes”) discusses the development of a SERS substrate using gold coated Multi-wall Carbon Nanotube on etched aluminum foil. Huge enhancements have been observed for both *in-vitro* and *in-vivo* process using this substrate.

Chapter 8 (“Substrate Enhanced Raman Scattering Substrate Using Gold Nano-particles on Thinned Silicon Wafer”) describes the fabrication of another SERS substrate by sputtering gold on the thinned silicon wafer. The wafer is thinning down using 30% KOH by one sided etching, and then gold is sputtered on the smooth side of the wafer. The reasons for thinning the wafer from 420 μ m to 120 μ m are explained there.

Chapter 9 (“Summary and Recommendations for Future work”) is as stated by its title.

CHAPTER 2: INTRODUCTION

2.1 Raman Scattering

"I propose this evening to speak to you on a new kind of radiation or light emission from atoms and molecules." Professor C. V. Raman started his lecture with the South Indian Science Association in Bangalore on March 16, 1928, in this way to his discovery i.e. Raman scattering [1, 2].

Raman scattering is an inelastic scattering of a photon, discovered by C. V. Raman (who was awarded The Nobel Prize in Physics in 1930), and later by K. S. Krishnan in liquids and G. Landsberg and L. I. Mandelstam in crystals. The effect had been predicted theoretically by Adolf Smekal in 1923. In 1998 the American Chemical Society designated Raman Effect as National Historic Chemical Landmark [3] for its analytical capability in molecular level in solids, liquids, and gases.



Figure 2.1. The first Raman spectrometer, built by C.V. Raman [1]

A monochromatic light (laser beam) is incident on a material and scattered in different directions. Scattering of this light can be divided into two types - Rayleigh scattering (named after British Physicist Lord Rayleigh) or elastic scattering, with no wavelength change and Raman scattering or inelastic scattering, with a change in wavelength. [4- 9]

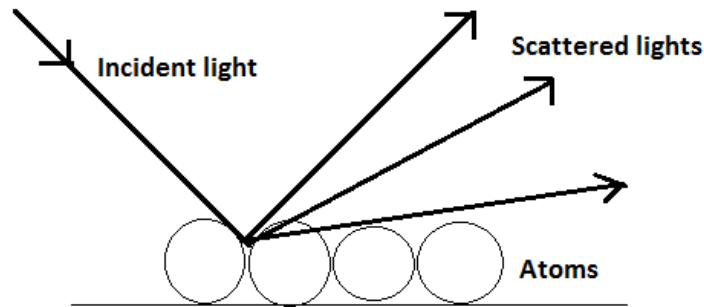


Figure 2.2. Incident light scattered in different directions

Approximately 1×10^{-7} of the scattered light is Raman. When a collision between the molecule of the sample and the laser beam (photon) occurs, three things can happen.

1. The energy and the wavelength of the incident photon and the scattered photon remain the same before and after the collision. As stated above, this is elastic scattering and known as Rayleigh scattering. Here, the frequency of the scattered light and incident light is also the same.

Therefore, the energy of the scattered light for is $E_s = E_i = h\nu$

(Where, h = Planck's constant, ν_s = Frequency of scattered light),

2. The energy of the scattered photon (E_s) is decreased in comparison to the incident photon due to absorption of energy by the molecule during the collision. This is inelastic scattering and is a type of Raman scattering. Here, the frequency of the scattered light is lower than the incident light, and the spectral line generated by this process is known as a Stokes line.

Therefore, the energy of the scattered light for Stokes line is $E_s = h\nu_s = (E_i - \Delta E)$

(ΔE = Energy difference between scattered light and incident light)

3. The energy of the scattered photon (E_s) is increased in comparison to the incident photon. This is also an inelastic scattering and is a type of Raman scattering. Here, the frequency of the scattered light is larger than the incident light, and spectral line generated by this process is known as an anti-Stokes line.

Therefore, the energy of the scattered light for Anti-Stokes line is $E_s = h\nu_s = (E_i + \Delta E)$

The probability of Stokes scattering is higher than Anti- Stokes scattering because anti-Stokes lines are generated only when the molecules are excited before irradiation [10]. Various types of scattering are shown in Figure 2.3.

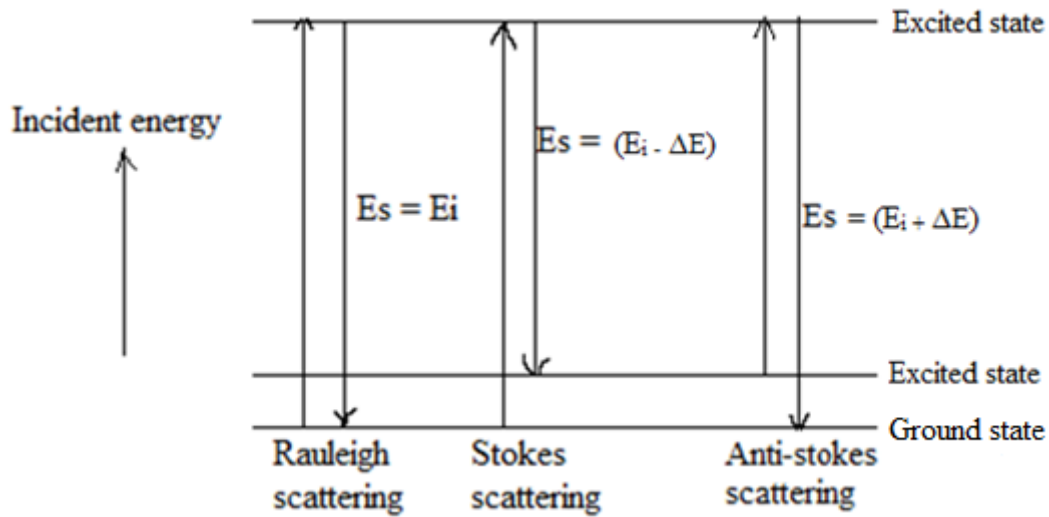


Figure 2.3. Rayleigh and Raman scattering

At room temperature, most of the atoms or molecules are in the ground state i.e. the lowest energy state and very few molecules are in excited states or higher energy state [3]. From Planck's equation (1), the wavelength changes with the change of energy of the photon.

$$E = h \nu \quad (1)$$

$$\nu = c / \lambda$$

(E= Energy of photon Joules, h= Planck's constant 6.626×10^{-34} J/s, ν = frequency Hz = 1/second)

$$E = h c / \lambda = 1.24 / \lambda \quad (2)$$

(c = Velocity of light = 3×10^{10} cm/s, λ = wavelength in μm , E = energy in eV)

The change in wavelength corresponds to a molecular excitation which in turns generates Stokes and anti-Stokes scattering. This is the quantum particle interpretation of Raman scattering, considering the light as a photon that collides with atoms and is scattered inelastically.

The Raman shift in the Raman Effect is the energy lost by the photon due to scattering. Using equation 1 and 2 it is found that,

$$\begin{aligned}
\Delta E &= E_i - E_s \\
&= h (\nu_1 - \nu_2) \\
&= h c \left\{ \left(\frac{1}{\lambda_1} \right) - \left(\frac{1}{\lambda_2} \right) \right\} \\
&= 1.24 \left\{ \left(\frac{1}{\lambda_1} \right) - \left(\frac{1}{\lambda_2} \right) \right\} \quad (3)
\end{aligned}$$

(λ_1 = Wavelength of laser beam, λ_2 = wavelength of scattered light)

Thus, from equation 3, the unit of Raman shift is cm^{-1} . It is also possible to explain the Raman Effect with classical wave interpretation, where the light is considered as an electromagnetic wave, which interacts with the atom through its polarizability [12]. A vibration of a molecule is generated when it absorbs energy, which in turn changes the covalent bond inside the molecule [11], and the molecular vibration interacts with the external oscillating electric field, which in turn generates induced dipole moment.

$$P = \alpha E \quad (4)$$

(P = induced dipole moment, α = polarizability of the molecule, E = external oscillating electric field)

$$E = E_0 \cos 2\pi \nu_0 t \quad (5)$$

(E_0 = the amplitude of the external oscillating electric field, ν_0 = frequency of the incident photon)

Therefore, $P = \alpha E = \alpha E_0 \cos 2\pi \nu_0 t$

$$\begin{aligned}
&= (\alpha_0 + \Delta\alpha \cos 2\pi \nu_\alpha t) (E_0 \cos 2\pi \nu_0 t) \\
&= \alpha_0 E_0 \cos 2\pi \nu_0 t + (\Delta\alpha \cos 2\pi \nu_\alpha t) (E_0 \cos 2\pi \nu_0 t) \\
&= \alpha_0 E_0 \cos 2\pi \nu_0 t + \frac{1}{2} \Delta\alpha E_0 \cos 2\pi (\nu_0 + \nu_\alpha) t + \frac{1}{2} \Delta\alpha E_0 \cos 2\pi (\nu_0 - \nu_\alpha) t \quad (6)
\end{aligned}$$

(α_0 = initial polarization, ν_α = molecule oscillating frequency, $\Delta\alpha$ = change rate of polarizability)

Thus, equation 6 shows that Rayleigh, Stokes and anti-Stokes scattering occur when light is incident on the substrate and scattered in different directions due to molecular vibration. The

shape of the Raman spectrum is constant for a specific molecule whereas the intensity of the spectrum can vary [13].

The advantages of Raman spectroscopy are given below [14, 15].

- (a) It is a non-contacting and moderately non-destructive process.
- (b) It can detect different chemical structures.
- (c) It can be used for almost all kinds of solids, liquids and gases.
- (d) Materials can be analyzed through glass, polymers and even in water.
- (e) Short sample preparation time.
- (f) Short measurement time.

In spite of all these advantages Raman spectroscopy has some disadvantages.

- (a) The Raman Effect is very weak, so the sensitivity is low.
- (b) Though it is considered to be a non-destructive process sample heating from a sufficiently high intensity laser beam can destroy the sample.

2.2 Raman Spectrometer

There are four major parts in a Raman spectrometer [15]

- a. Excitation Source (typically a Laser)
- b. Sample illuminating system and light collection optics
- c. Wavelength selector (Notch filter and Diffraction grating)
- d. Detector (Charge-coupled device)

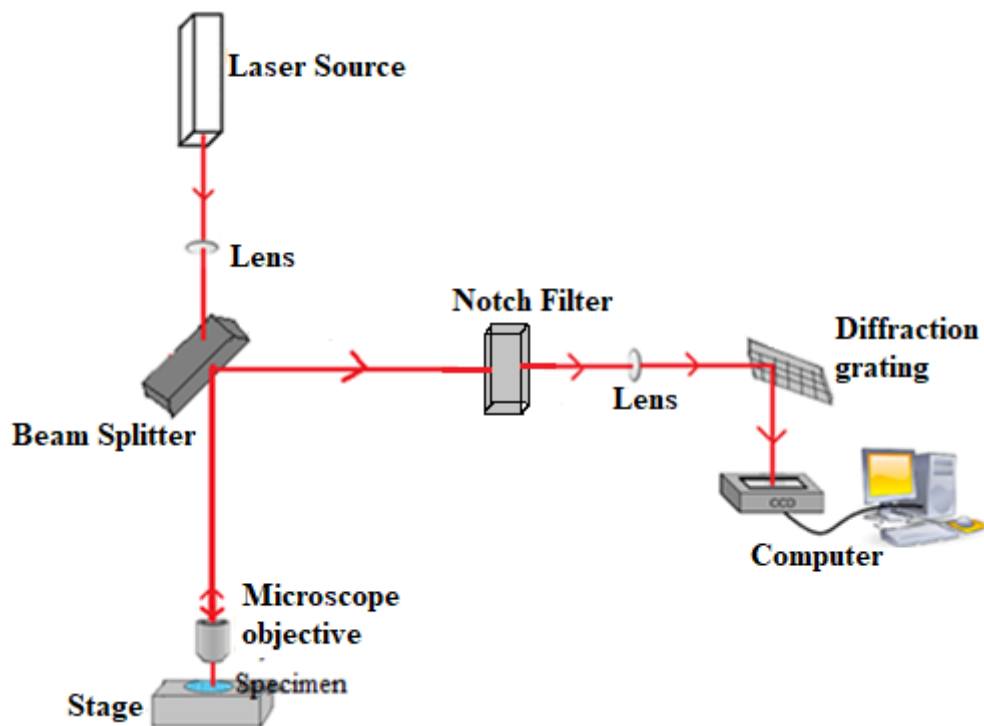


Figure 2.4. Schematic diagram of a Raman Spectrometer

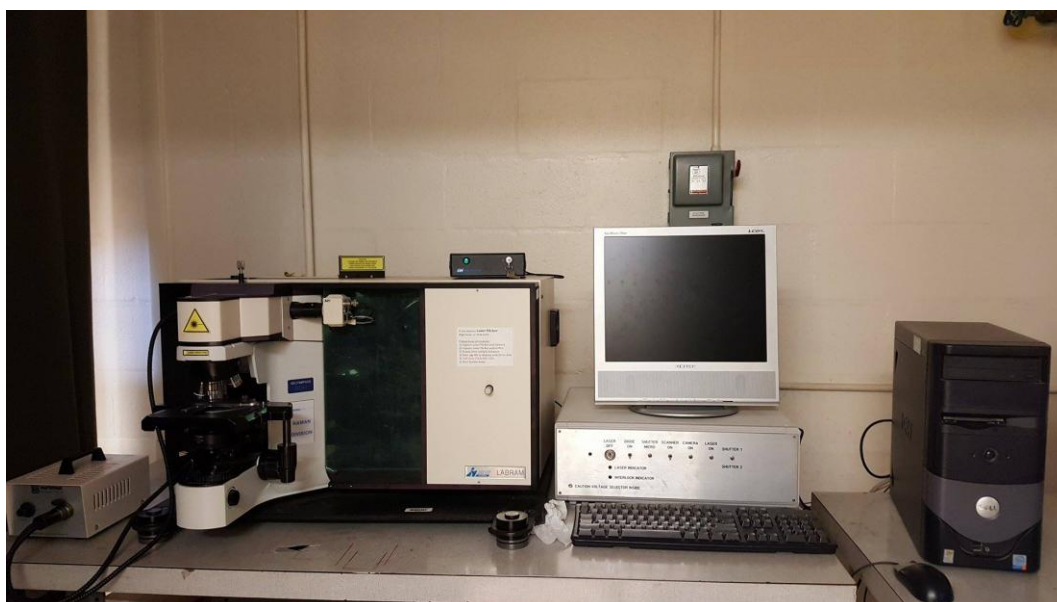


Figure 2.5. LABRAM Raman spectrometer at EMDL in LSU

The Raman spectrometer shown in Figure 2.5 is a LABRAM LAB300 visible/infrared with a confocal microscope. The microscope is equipped with different objectives: 10X (Numerical Aperture= 0.30 and Working Distance=10.10mm), 50X (Numerical Aperture= 0.50 and Working Distance=0.66mm), 50X (Numerical Aperture= 0.55 and Working Distance=10.00mm), 100X (Numerical Aperture= 0.90 and Working Distance=0.21mm). The wavelength of its He-Ne laser is 632.81nm.

2.3 Surface Enhanced Raman Scattering (SERS)

There are many ways to increase the Raman intensity [16]. Surface enhanced Raman Scattering (SERS) broadens the use of Raman spectroscopy for more applications. It was discovered by Martin Fleischmann, Patrick J. Hendra, and A. James McQuillan at the Department of Chemistry at the University of Southampton, Southampton, the UK in 1973 [17,18]. The SERS effect can increase weak Raman signals by factors of up to 10^6 - 10^{10} [19], so weak signals can be detected by the enhanced Raman signals. There are two mechanisms by which this enhancement occurs.

1. Electromagnetic enhancement – Due to the rough surface of the metal surface the laser beam excites electrons from the surface and creates plasma resonance and strong enhancement of the electric field [20, 21]. The maximum enhancement of the electric field occurs across small gaps when the plasmon frequency is in resonance with the laser frequency, and scattering will occur only when the plasmon oscillates perpendicular to the surface [22]. It is highly dependent on the surface geometry.

2. Chemical enhancement - This enhancement occurs due to the bond formation or charge transfer between the metal surface and the adsorbed molecule (molecule adsorbed in the metallic structure which is in nm range). [23, 24]

Among these two enhancements, electromagnetic enhancement is dominant in SERS and plasma resonance at the surface is the main reason for that. The enhancement factor (EF) of SERS is given below.

$$EF = (I_{SERS} * N_{RS}) / (I_{RS} * N_{SERS}) \quad (7)$$

(I_{RS} is the intensity of the normal Raman spectra, I_{SERS} is the intensity of the enhanced Raman spectra, and N_{RS} is the number of molecules involved in the normal Raman spectra, and N_{SERS} is the number of molecules involved in the enhanced Raman spectra)

2.4 Materials used for Surface Enhanced Raman Scattering (SERS)

Usually, gold (Au), silver (Ag) or copper (Cu) are used [25] for SERS as they are highly conductive, and their plasmon resonance frequencies, depending on the geometry of the substrates, are in the visible and near-infrared frequency range. Aluminum is also used. The plasmon resonance frequency of aluminum includes the ultra violet range which is not true for gold, silver or copper. In addition, aluminum shows enhancement in the infrared frequency range. [22].

Table 2.1 Plasmon resonance wavelength for gold, silver, copper, and aluminum [22]

Materials	Wavelength range (nm)
Gold (Au)	580-1250
Silver (Ag)	400-1000
Copper (Cu)	550-1250
Aluminum (Al)	300-1000

Rough metal surfaces are created by distributing nano particles on the substrate by sputtering, lithography, electrospinning, electrochemical deposition, etc. The size and the shape of metal nano particles are directly related to the enhancement factor of Raman scattering. Thin metal film creation is another process of developing a metal surface on the substrate.

We choose Gold (Au) over Silver (Ag) for the following reasons -

1. Gold is non-toxic [26] whereas silver can be toxic. In this work, the enhancement probe may enter the human body. So, toxic material can't be used.
2. In fabricating the probe, some materials have to be etched. Gold lasts longer than silver in most etches.
3. Ordinarily, silver does not react with oxygen. But, if sulfur compounds are present in the air then it reacts slowly and creates silver sulfide (Ag_2S), a black compound. But, gold is unaffected by air, water, alkalis and all acids. It dissolves only on aqua regia (a mixture of hydrochloric acid and nitric acid).

Therefore, for this research purpose gold is more useful and stable than silver.

CHAPTER 3: MOTIVATION AND RESEARCH GOALS

In Raman spectroscopy a small fraction of the light scattered by the sample generates a unique "fingerprint" of the material. But, the signal is very weak. In order to enhance the intensity of the Raman signal the concept of surface enhanced Raman spectroscopy (SERS) has been developed several years ago. Rough nano- metallic structures are needed to enhance the signal. Generally, SERS substrate helps to increase the intensity by a factor of 10^6 to 10^9 . The development of a low-cost, high sensitive SERS substrate and using it not only for the chemical specimen detection but also for the detection of biological specimen is the main motivation behind this work.

Often biopsies are performed to detect cancer in tissue. But, they increase post procedural risks at the suspected cancer section, and they are time-consuming as well. So, in clinical applications it is desirable to obtain the Raman signal from within a remote specimen, with a probe which is minimally invasive, low cost, less time consuming and reusable with no post procedural risk.

A desirable SERS probe would be thin, less invasive, and produce a strong SERS signal. This can be achieved with a narrow probe that is remotely coupled to the Raman spectrometer. It is desirable for the signal to be enhanced. In this work a Surface Enhanced Raman Scattering (SERS) probe is developed. An optical fiber would provide a flexible coupling between the probe and the spectrometer. But, a fiber more than a few centimeters long generates its own Raman signal, which masks the signal from the specimen. In this work, 3 different low cost, high sensitive SERS substrates have been developed, which contain nano-rough metallic surface ideal for the enhancement purpose.

This research work has the following goals:

- 1) Preparation of a low-cost nano structured SERS template based on aluminum foil and gold
- 2) Attaching the nano rough gold to the end of an optical fiber
- 3) Preparing a probe in a 0.5mm outside diameter needle containing a gold coated optical fiber
- 4) Connecting the probe to the spectrometer by a 1m long air path in an articulated mirrored arm
- 5) Identifying different biological tissues
- 6) Development of a highly sensitive SERS substrate using gold coated multi-wall carbon nanotubes on etched aluminum foil, and
- 7) Development of another low-cost SERS substrate by sputtering nano-gold particles on thinned silicon wafer.

CHAPTER 4: NANO COST SURFACE ENHANCED RAMAN SCATTERING (SERS) SUBSTRATE USING ALUMINUM FOIL AND GOLD

4.1 Introduction

Household aluminum (Al) foil was used to prepare a SERS substrate in this work. A Scanning Electron microscope (SEM) was used to observe the surface morphology and the topography of this SERS substrate [29].

4.2 Raman Methods

There are two types of applications in SERS measurements: *in vitro* (conventional method) and *ex vivo* (Probe).

In the *in vitro* method, the laser beam typically passes through a transparent specimen in contact with the rough metallic surface. Figure 4.1 shows the conventional method of SERS. The specimen could be solid or liquid.

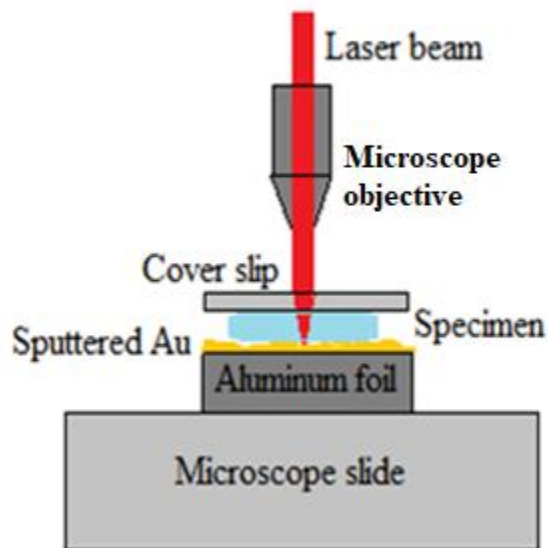


Figure 4.1. *In Vitro* / Conventional method of SERS

In the *ex vivo* process, the laser beam passes through the rough metallic surface. Figure 4.2 shows the *ex vivo* probe used with a dummy specimen.

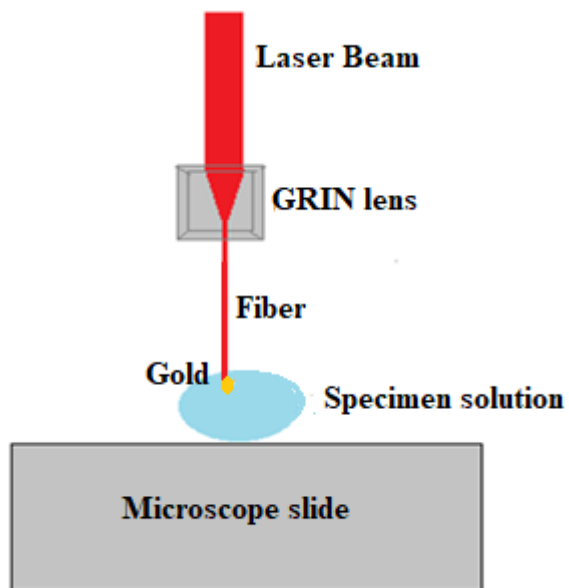


Figure 4.2 *Ex Vivo* SERS Probe

4.3 Specimen Preparation

4.3.1: Rhodamine 6G Solution Preparation

Transparent specimens were used to measure the *in vitro* enhancement produced by the aluminum gold based SERS substrate. Rhodamine 6G (R6G) solution is a widely used specimen for SERS [35- 38]. The chemical formula of R6G is $C_{28}H_{31}N_2O_3Cl$. The chemical structure of R6G is shown in Figure 4.3.

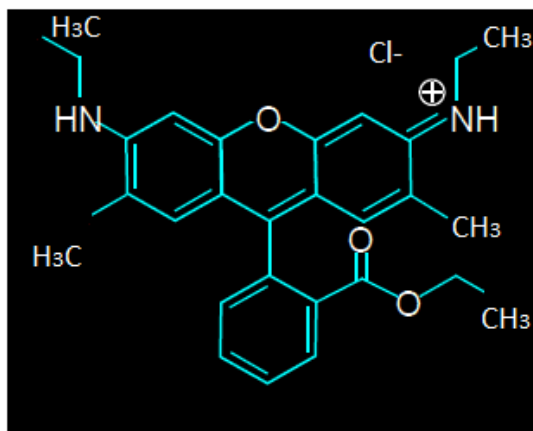


Figure 4.3. Chemical structure of Rhodamine 6G

The molecular weight of R6G is 479.01 g/mole, and the solubility is 20g/L at 25⁰C temperature [29]. For this research R6G powder was dissolved in DI water at room temperature and concentrations varied from 1nM to 1mM by factors of 10 were prepared, shown in Figure 4.4. The 1mM solution is dark red, 100 μM is orange, and 10 μM is pinkish. The 1 μM is almost transparent, and 100nM to 1nM are clear.



Figure 4.4. Different concentrations of R6G solutions for *in vitro* measurements

4.3.2: Gelatin using Rhodamine 6G Solution Preparation

For *ex vivo* like measurements gelatin samples were prepared with different concentration of R6G solution (Figure 4.5). 500mg of gelatin (Knox unflavored gelatin, Kraft Foods Global, Inc.) was mixed with 5ml of the R6G solution to prepare gelatin blocks. The mixture was heated to 50-60 °C temperature and stirred continuously until the gelatin powder dissolved completely. Then it was left under a chemical hood at room temperature for 6 hours so that it solidified completely. Gelatin was used for this research as it is comparable with the human tissues [40], transparent and easy to prepare.



Figure 4.5. Gelatin prepared with different concentrations of R6G solutions varying from 1nM to 1mM for *ex vivo* like measurements

4.4 Substrate Preparation

4.4.1: Substrate Cleaning

The Al foil was cleaned by rinsing in acetone, isopropyl alcohol (IPA) and DI water. It was then dried in nitrogen gas. Acetone washes away organic materials on the aluminum, but leaves some residues. IPA removes those residues plus greasy materials on the substrates.

4.4.2: Etching of Aluminum Foil

The foil was etched for 1 minute at room temperature in 30% Potassium hydroxide (KOH), followed by a DI water rinse and nitrogen gas drying. Approximately 1 μm thickness of

aluminum was removed by this isotropic etching, measured by Alpha Step. To prepare the KOH solution 70 grams of KOH pellets were mixed in 230mL of de-ionized (DI) water at 25⁰C temperature [31, 32]. Signals were obtained from both front and back side of the non-etched, etched, and etched while stirring Al foil using 1mM R6G solution as a specimen (table 2). The 50X microscope objective (NA= 0.55) was used to do the measurements. For each case, the laser beam from the spectrometer was focused at the junction of the gold layer and specimen.

Table 4.1 Raman intensities of 1mM R6G solution on different types of aluminum foil without gold on both the front and the back side

Different types of Al foil on both side without gold	Raman Intensity of 1mM R6G
1. Non-Etched AL foil Front	178
2. Non-Etched AL foil Back	232
3. Etched (for 60sec) AL foil Front	207
4. Etched (for 60sec) AL foil Back	265
5. Stirred Etched AL foil Front	230
6. Stirred Etched AL foil Back	282

Household aluminum foil is 98.5% - 99.9% pure aluminum. Available aluminum pellets are 99.9999% pure aluminum. The foil and the pellets produced similar Raman spectra (Figure 4.7).

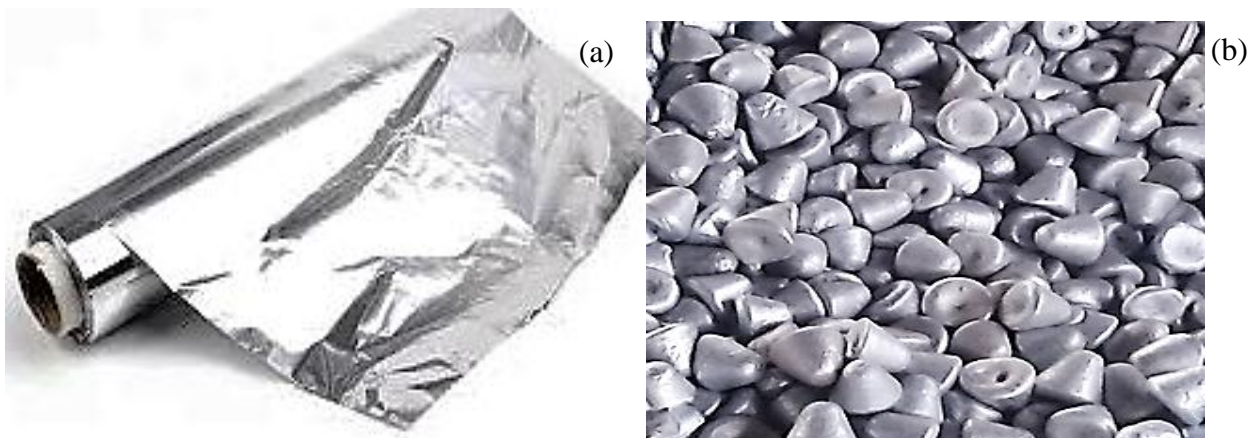


Figure 4.6. (a) Photograph of the Aluminum foil (98.5% - 99.9% pure aluminum), (b) Photograph of the Aluminum pellets (99.9999% pure aluminum)

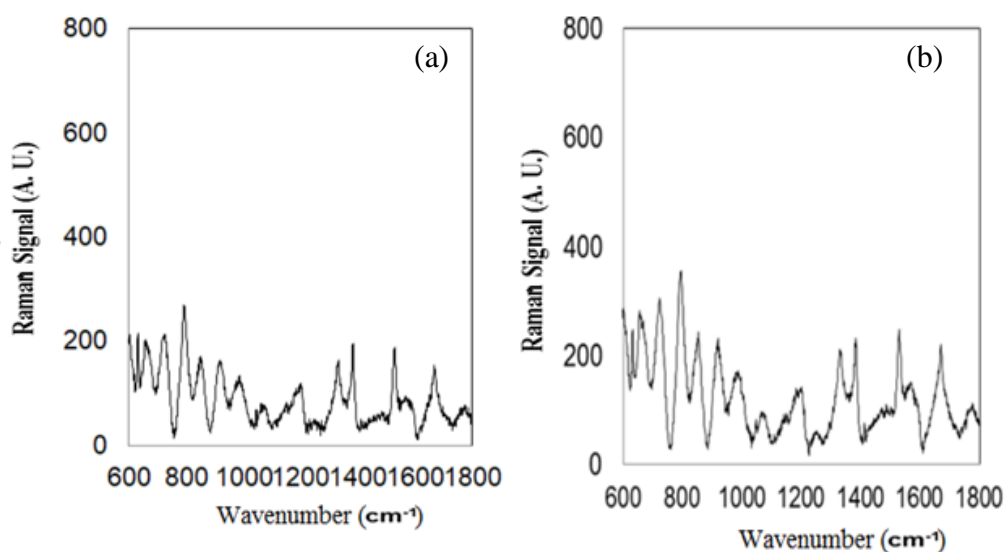


Figure 4.7. (a) Raman spectrum of the non-etched Aluminum foil, (b) Raman spectrum of the non-etched Aluminum pellet

Results for pellets in 1mM R6G solution are shown in Table 4.2. 60 sec etching time was optimum for enhancement. Etching the aluminum pellet creates a rough surface (in nano scale range), which helps to enhance the Raman signal. The stirring based etching showed only a little

enhancement compared to normal etching. So, it was decided to sputter gold on all the aluminum samples to check the enhancement.

Table 4.2. Raman intensities of 1mM R6G solution for different etching times to determine the optimum etching time for enhancement

Type of Pellets	Raman intensity of 1mM R6G solution
1. Non-Etched Pellet	205
2. Etched AL Pellet 10s	228
3. Etched AL Pellet 30s	276
4. Etched AL Pellet 60s	310
5. Etched AL Pellet 120s	192

4.4.3: Gold Deposition on Substrate

Stronger enhancements were obtained by sputtering gold (Au) of thickness 20nm on the foil. Previous work [33] showed that 20nm gold thickness is best for enhancement purpose. Sputtering was done by a DC powered magnetron (Oxford Plasma lab System 400 sputtering system), at CAMD, LSU. A 2-5 kV DC voltage, a high vacuum of 10^{-6} Torr, and argon gas created a neutral plasma within the system. [34] The plasma contains electrons and argon ions. Argon ions accelerate towards the target due to the applied potential. The argon ions bombard the gold target and neutral gold atoms are ejected which deposit on the aluminum substrate. A schematic diagram of the DC powered magnetron sputtering tool is shown in Figure 4.8.

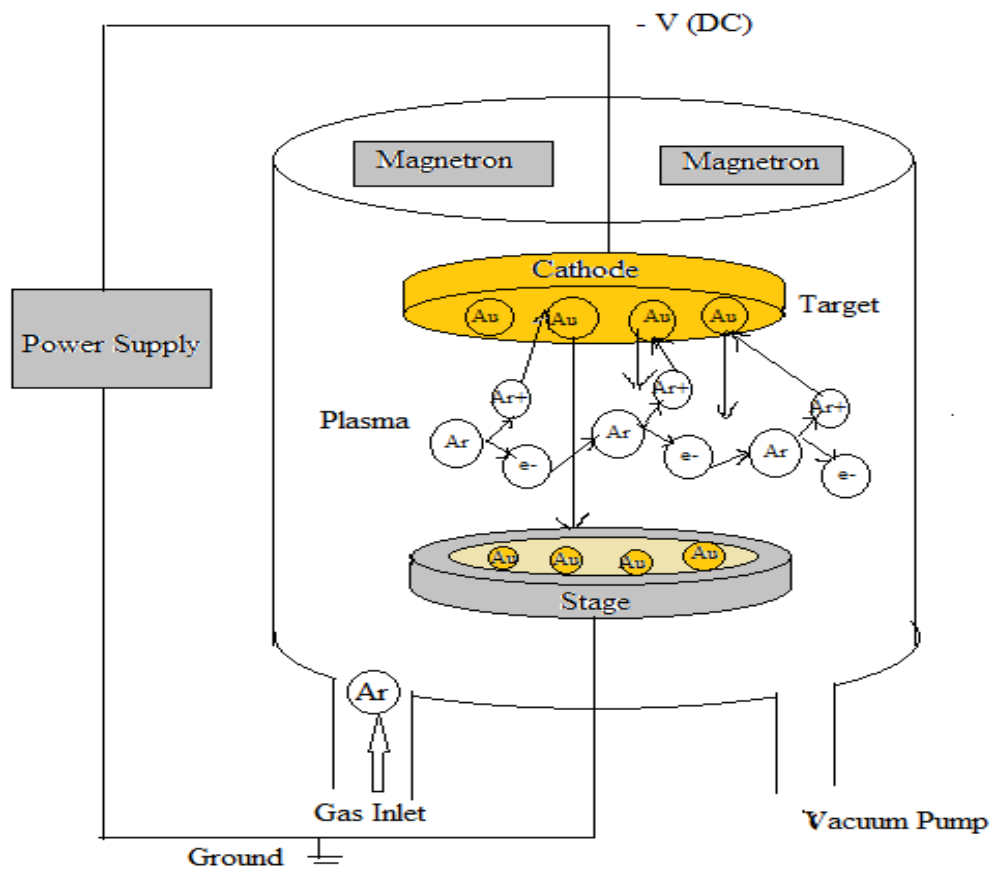


Figure 4.8. Schematic diagram of the DC powered magnetron sputtering machine

Gold was sputtered on 6 different samples of Al foil, keeping the sputtering condition fixed for all of them. Table 4.3 shows the enhancement caused due to gold on different Al foil using 1mM R6G solution as a specimen.

Table 4.3. Raman intensities of 1mM R6G solution on different types of aluminum foil with gold on both front and back side

Different types of Al foil with 20 nm of gold	Raman Intensity of 1mM R6G solution
1. Non-etched Al foil Front	672
2. Non-etched Al foil Back	374
3. Etched (for 60s) Al foil Front	1358
4. Etched (for 60s) Al foil Back	1552
5. Stirred Etched (for 60s) Al foil Front	4277
6. Stirred Etched (for 60s) Al foil Back	11693

Stirring based etched (for 60 sec) aluminum foil with 20nm sputtered Au on the back had the greatest enhancement. This substrate was chosen for the SERS probe. Sputtering creates small islands of closely packed gold nanostructures, which are ideal for enhancement (Figure 4.9).

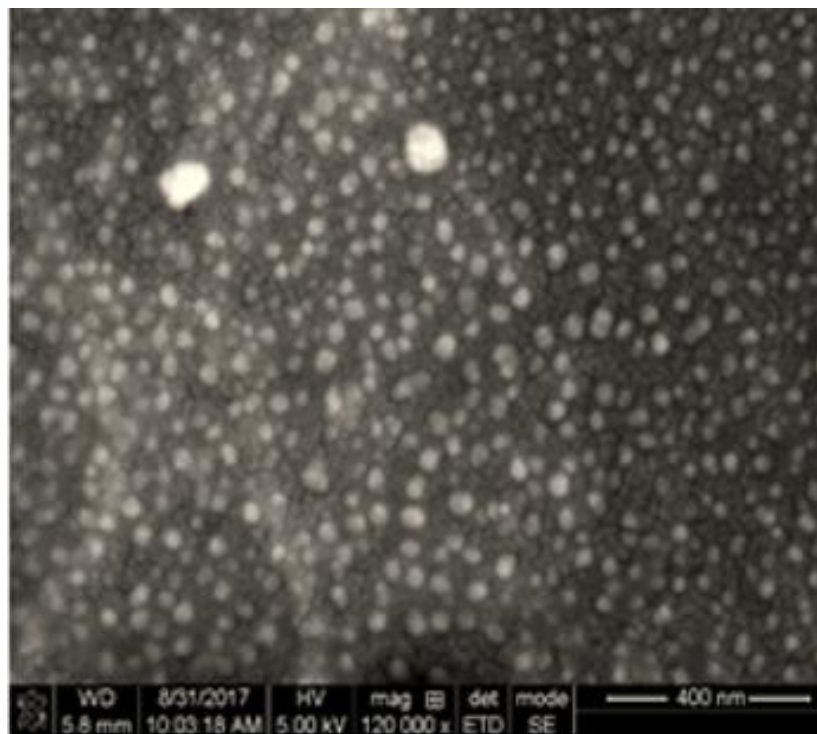


Figure 4.9. SEM image of sputtered gold on back side of the stirring etched aluminium foil

In order to check the performance of the aluminium foil based SERS substrate for the *in-vivo* like method the SERS substrate was epoxied to a microscope slide with the gold surface facing the slide. The aluminium foil was etched out completely using 30% KOH solution at room temperature. The laser beam was focused at the junction of the R6G solution and gold through microscope slide, epoxy and gold. The intensity of the Raman spectrum smaller compared to what was obtained for the in-vitro method for the same SERS substrate. The spectrum for different concentrations of R6G solution varying from 1nM to 1mM is obtained using this process (Figure 4.10). The spectrums are shown in Figure 4.11. By change of factor of 10^6 in concentration, the intensity is changed by a factor of 10. So, we can say the lower signal concentration is increased approximately by a factor of 10^5 due to this SERS substrate.

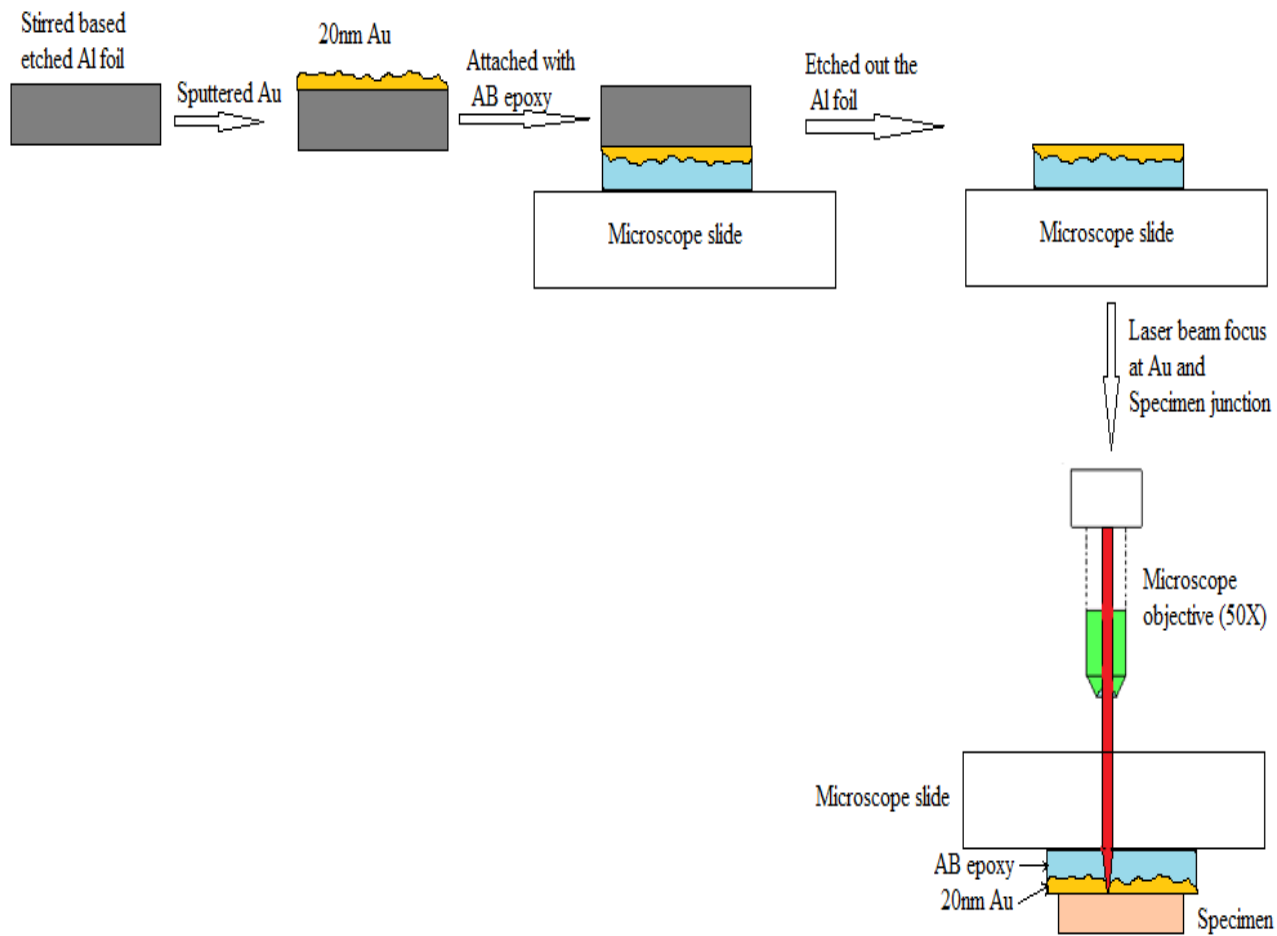


Figure 4.10. Process of obtaining Raman signal using *ex vivo* like method

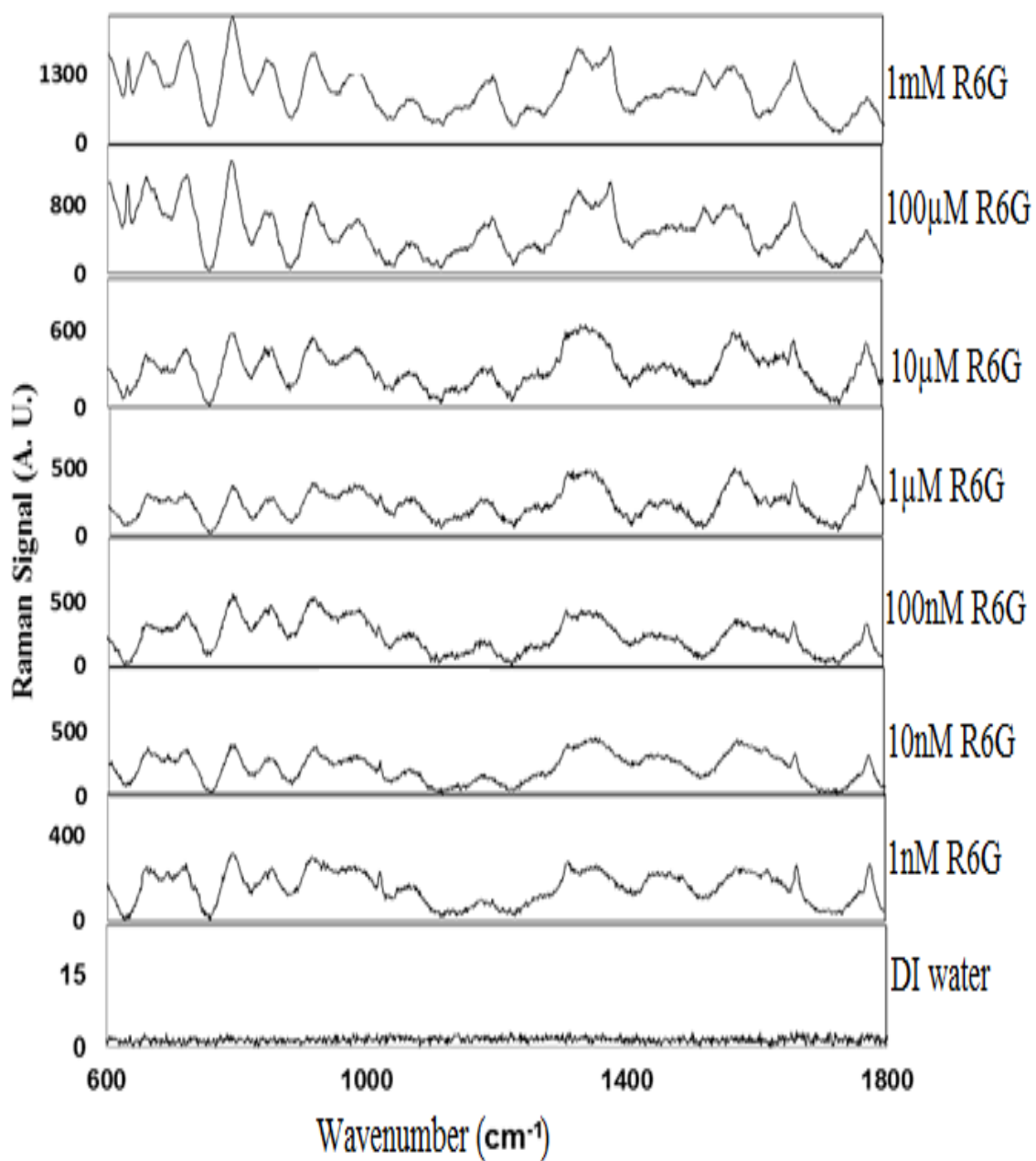


Figure 4.11. Raman spectrum of DI water and R6G solutions (concentration varies from 1nM to 1mM by a factor of 10) using *ex vivo* like method.

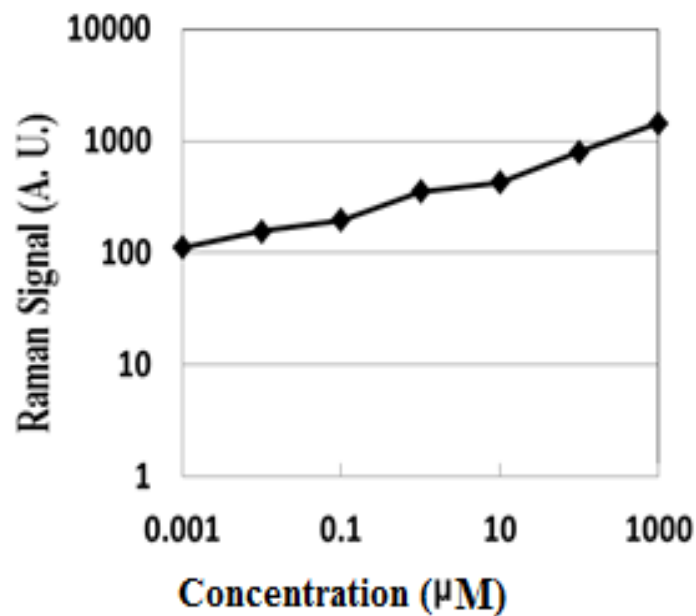


Figure 4.12 Raman signals (using 50x microscope objective) for viewing through gold as a function of the concentration of R6G solutions

4.5 Conclusions

This chapter described fabrication of a low cost Surface Enhanced Raman Scattering (SERS) substrate. The chemical specimen preparations for both *in vitro* and *ex vivo* like method were described along with the Raman spectrum using those specimens for both the methods.

CHAPTER 5: SINGLE FIBER BASED SURFACE ENHANCED RAMAN SCATTERING (SERS) PROBE DESIGN

5.1 Introduction

In some cases, e.g., clinical applications, it is desirable to obtain a Raman signal from within a remote specimen. This can be done with a narrow probe that is remotely coupled to the Raman spectrometer. [11, 33, 41-42] In principle such a probe could consist of a single optical fiber.

In practice, however, an optical fiber more than a few cm long generates its own Raman signal. This effectively masks the signal from the sample. Consequently, previous SERS probes have used separate laser and spectrometer fibers. [43-45] However, probes with two fibers are inherently far less sensitive than single fiber probes.

This work compares one and two fiber probes and describes how a single fiber probe can avoid the masking background signal and produce a signal comparable to that of a sample on the microscope stage.

Some sections of this chapter in its current form are published in a journal article. It is reproduced with changes from [Srismrita Basu, Hsuan-Chao Hou, Debsmita Biswas, Subhodip Maulik, Theda Daniels-Race, Mandi Lopez, Michael Mathis, and Martin Feldman, "A needle probe to detect surface enhanced Raman scattering (SERS) within solid specimen", *Review of Scientific Instruments*, 88(2), 2017] with the permission of AIP Publishing (Appendix A)

Some sections of this chapter in its current form are published in a journal article. It is reproduced with changes from [Srismrita Basu, Hsuan-Chao Hou, Debsmita Biswas, Theda Daniels-Race, Mandi Lopez, Michael Mathis, and Martin Feldman, "A Single Fiber Surface Enhanced Raman Scattering (SERS) Probe", *Journal of Vacuum Science & Technology B, Nanotechnology and Microelectronics: Materials, Processing, Measurement, and Phenomena*, 35(6), 2017] with the permission of JVSTB Publishing (Appendix B)

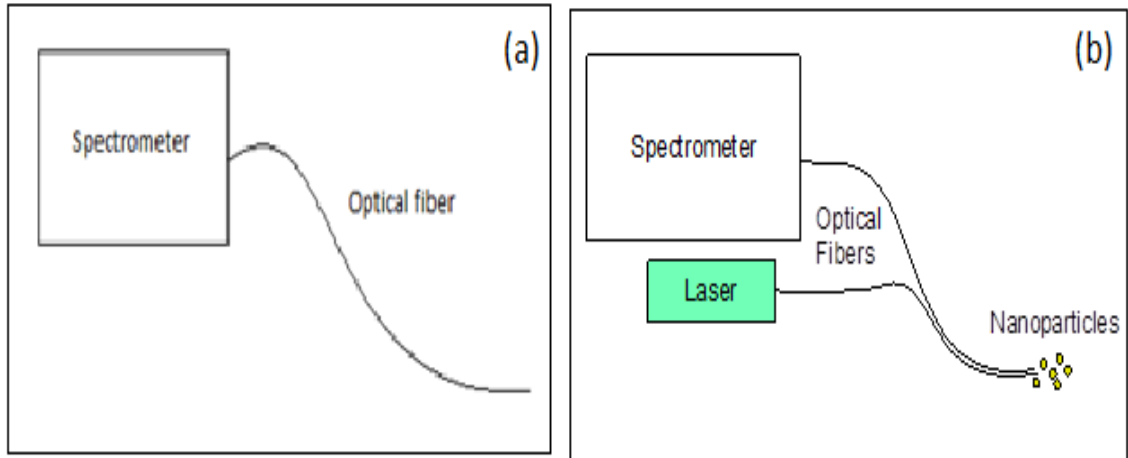


Figure 5.1. (a) Long single fiber system, (b) Two fiber system

5.2 Theory

The SERS signal originates within a few nanometers of the rough metallic surface. The amount of Raman light that is captured is proportional to the solid angle through which it is viewed. In a conventional system, a microscope objective is focused on the metallic surface. The signal strength at focus is proportional to the solid angle sustained by the objective or to the square of its numerical aperture NA

$$S_R = C (NA)^2 \quad (7)$$

(S_R = Raman signal strength and C = a constant)

Table 5.1 given below shows the data for different microscope objectives with different numerical apertures to calculate the relation between Raman intensity and numerical aperture. These data were then plotted to show that Raman intensity is proportional to the square of the numerical aperture (Figure 5.2).

Table 5.1. Raman intensity for different microscope objectives and Probe with different numerical apertures

Objective	NA	Raman intensity
2.5X	0.075	200
4X	0.10	600
Probe	0.12	460
10X	0.25	2900
10X	0.30	3500
50X	0.55	14000

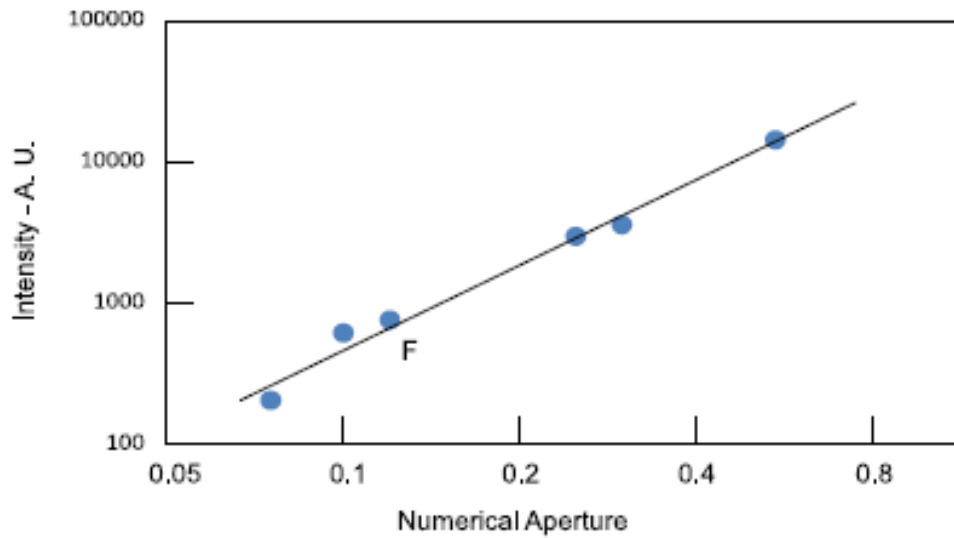


Fig. 5.2. Surface Enhanced Raman signal strength as a function of numerical aperture. Except for point "F", all the data were taken through microscope objectives focused on the same rough metallic sample. F was taken through an optical fiber, and the data has been compensated for a 50% insertion loss. The straight line is a fit to Raman intensity proportional to the square of the Numerical Aperture. [46]

The signal strength is independent of the focused spot size, which is always small compared to the objective's lens diameter. The signal strength depends on the focus. However, the conventional formula for depth of focus,

$$\text{DOF} = k_2 \lambda / (\text{NA})^2 \quad (8)$$

where k_2 is a constant close to 0.5, cannot be used because the incident laser beam does not fill the microscope objective.

The entrance slit of the spectrometer is nominally conjugate to the focus of the microscope objective. Depending on the signal strength vs. resolution tradeoff made by the manufacturer, out of focus Raman light may overflow the entrance slit and be lost. Empirically it is found that the depth of focus in our spectrometer is about 9 μm FWHM for an $\text{NA} = 0.55$ objective, compared to about 1.3 μm as predicted by Equation (7) (Figure 5.3).

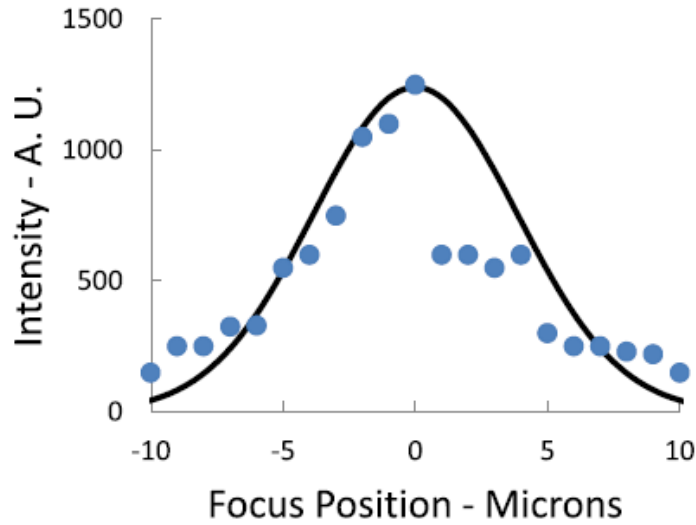


Figure 5.3. Surface enhanced Raman scattering signal strength as a function of focus for a 50X, $\text{NA} = 0.55$ microscope objective. A Gaussian fit is shown for comparison. The FWHM is roughly 9 μm , much larger than the nominal depth of focus of the objective. [46]

In addition to a potential reduction in probe diameter, a single optical fiber has an important advantage in signal strength over two adjacent fibers. The light exits a single mode fiber at a waist, corresponding to the waist formed at the focus of a microscope objective of the same NA. A metallic surface on the end of the fiber is in perfect focus, and the Raman light is collected within the NA of the fiber. There is a different situation in probes that use two fibers (Figure 5.4).

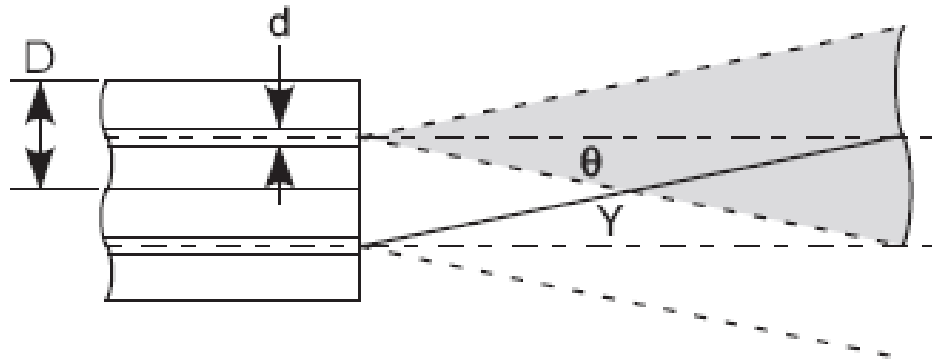


Figure 5.4. A two-fiber SERS system. Single mode laser light exits the top fiber, interacts with nanoparticles in the shaded region, and generates Raman light which enters the bottom fiber in the zero order. [46]

Single mode laser light exits the top fiber with a numerical aperture $\sin(\theta)$ into a cone of half angle θ . Nanoparticles are distributed in the region to the right of the fibers. Raman signals from the nanoparticles can only enter the bottom fiber signals as single mode light if they originate in the region where the NA's of the two fibers overlap. For simplicity, we assume that the nanoparticles are concentrated in the plane where the NA cone of the top fiber meets the center line of the bottom fiber. About 40% of the laser beam lies within the NA cone of the bottom fiber. The distance to the core of the bottom fiber, Y , is

$$Y = D / \sin\theta \quad (9)$$

The effective numerical aperture for Raman light entering the bottom fiber is related to the entrance diameter and the distance to the fiber,

$$\text{NA (entrance)} = d/2Y \quad (10)$$

From Equation (7), the ratio, R, of signal strengths is proportional to the square of the numerical apertures. Thus the ratio of the signal strengths between a single fiber of numerical aperture $\sin(\theta)$ and a two-fiber system with NA given by Equation (9) is

$$R = (2D/d)^2 \quad (11)$$

For our fibers, $D = 125 \mu\text{m}$ and the core diameter, $d = 5 \mu\text{m}$, so that $R = 2500$. The two fiber signals are further reduced because only 40% of the laser light contributes, losses in the tissue between the fiber and the nanoparticles have been neglected, and the dispersed nanoparticles may be less effective in generating hot spots than the closely packed nanoparticles on the end of the single fiber. Although to some extent this large ratio can be mitigated by reducing the fiber diameters, and/or using multiple Raman fibers or directing the NA cones toward each other, [47- 49] there still remain the problems, in a clinical setting, of introducing the nanoparticles, comparing sites with different nanoparticles, and either removing the nanoparticles or letting them remain in the subject.

The advantages of a single fiber probe are maintained if the fiber is only a few cm long. This short fiber can be coupled to the spectrometer through a long air path via an articulated mirrored arm. [33, 41] The data point labeled “F” in fig. 17 was obtained with a 5 cm long optical fiber of $\text{NA} = 0.12$ coupled to the air path with an integral Graded Index (GRIN) lens. The data have been adjusted by a factor of 2 to compensate known insertion losses in the path from the spectrometer to the GRIN lens.

5.3 Experimental

Gold is a desirable enhancement metal in a clinical probe, [50] since it is non-toxic, non-reactive, etch resistant, highly conductive, and almost transparent in thin depositions. However, it adheres very poorly to glass, and recent work has sought a suitable adhesion layer for SERS applications. [51] Instead of seeking to bond deposited gold directly [52- 54] to the glass fiber, we have exploited a related property: on many surfaces, a thin layer of deposited gold forms closely packed nano sized beads, like drops of water on a glass sheet.

Probe construction starts by sputtering a layer of gold nominally 20 nm thick, which is deposited as an array of nanoparticles, on a sheet of household aluminum foil.

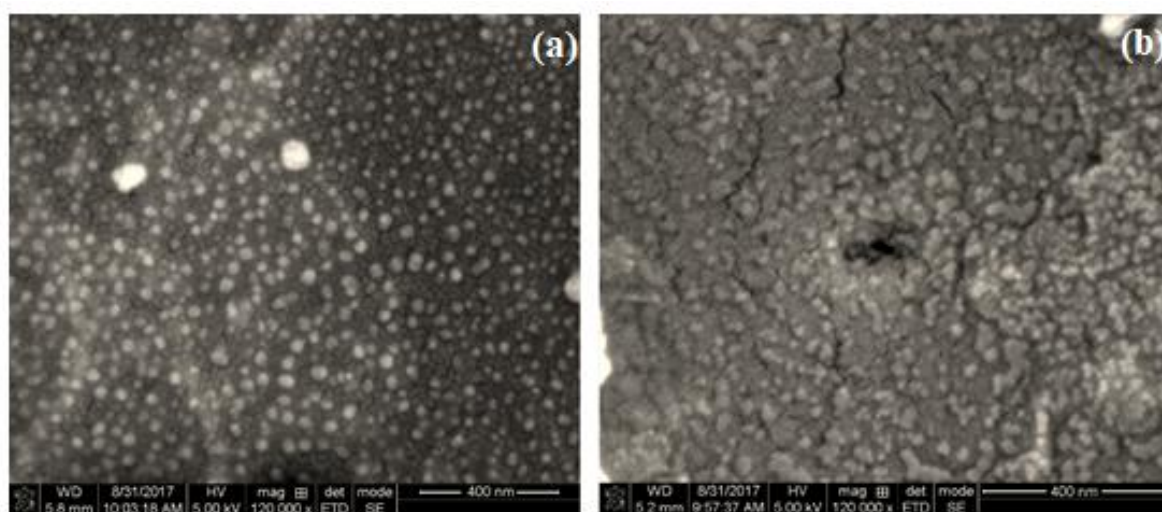


Figure 5.5 (a) SEM image of 20 nm of sputtered gold on aluminum foil. (b) SEM image of 20 nm of gold after epoxying to glass and etching away the aluminum. The characteristic closely packed gold globules form an ideal surface for enhancing Raman scattering. [55]

The fiber is a component of a commercially available GRIN lens assembly (GRIN Fiber Collimator model 50-630, Thor labs, Newton, NJ) (Figure 5.6).

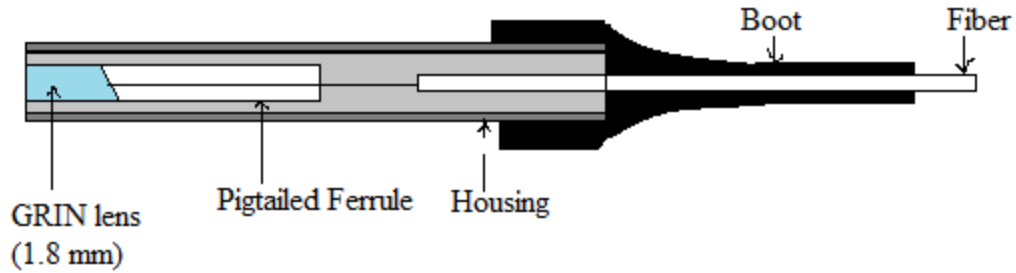


Figure 5.6. Schematic diagram of the GRIN lens coupled fiber

The fiber of this assembly was cleaved to length and the jacket removed for about 1 mm from the end of the fiber (Figure 5.7(a)). Stainless steel tubes, telescoping down to 0.5 mm outside diameter, were epoxied in place between the GRIN lens and the fiber (Figure 5.6(b)), leaving about 20 μm of fiber protruding from the end. The aluminum foil, gold side up, was placed on a compliant rubber block (Figure 5.7(c)). A small amount of quick setting clear epoxy was placed on the aluminum foil, and the probe was forced down with sufficient pressure to produce a permanent dent in the rubber and drive any excess epoxy from the gap between the fiber and the gold. After the epoxy had fully hardened, the aluminum was removed by etching in a 6% KOH solution at room temperature for 2 hours. Excess epoxy was removed by hand sanding with 400 grit sandpaper (Figure 5.7(d)). A photo of the finished probe is shown in Figure 5.7(e). It is estimated that because of the pressure during bonding, less than about 1 μm of epoxy was left between the end of the fiber and the gold nanoparticles.

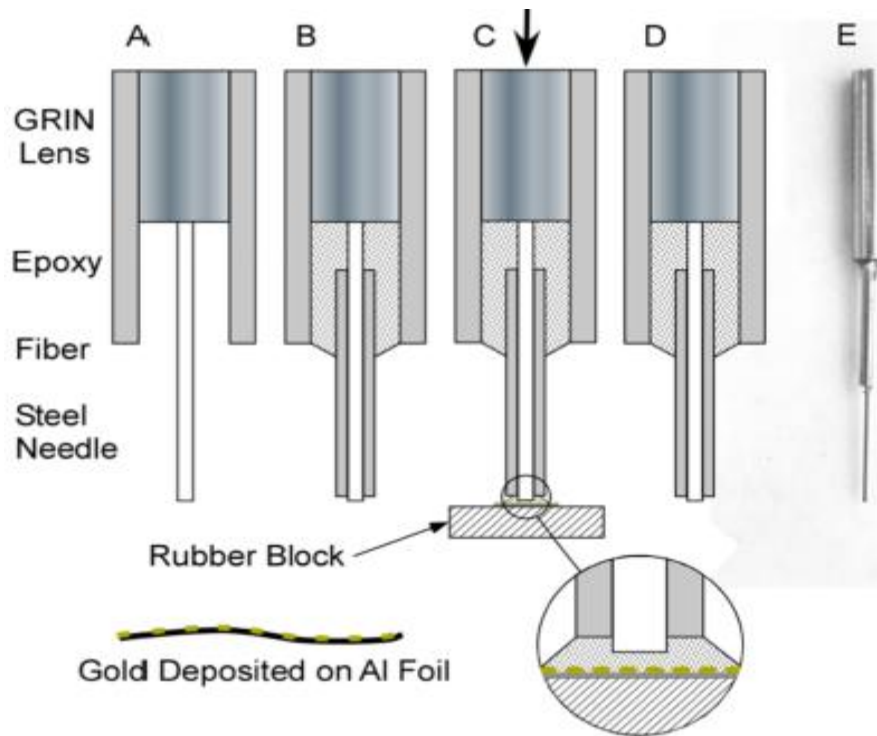


Figure 5.7. (a) Simplified sketch, not to scale, of GRIN lens and optical fiber assembly. For clarity, the fiber jacket, etc., have been omitted (b) Stainless steel needle epoxied in place (c) Gold covered foil epoxied under pressure to the fiber (d) Aluminum dissolved in etch, leaving a thin layer of gold epoxied to the fiber (e) Photograph of the finished probe. [46]

Another probe was prepared by thinning down the cladding of the optical fiber. For that purpose, the optical fiber was inserted vertically in hydrofluoric (HF) acid for 6 hours, which reduced the cladding diameter from 125 μm to 50 μm . Only the end of the fiber approximately 50 μm long was thinned. The optical image of the side view of the optical fiber before and after etching is shown in Figure 5.8.

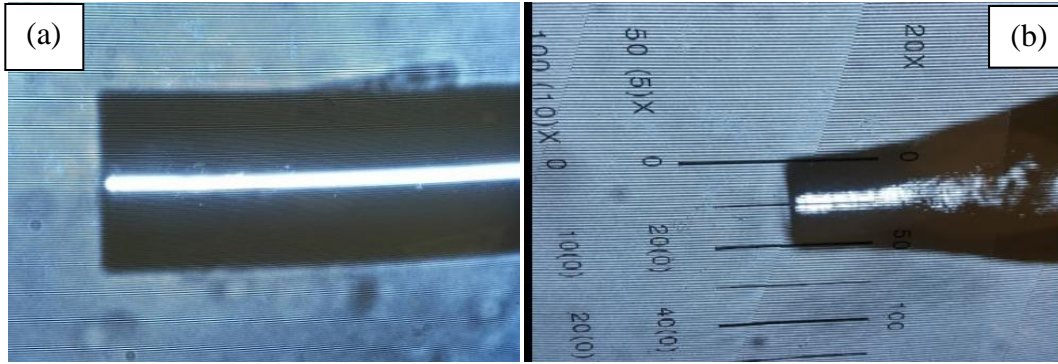


Figure 5.8. (a) Side view of the fiber before etching under 20X microscope objective, and (b) side view of the fiber after etching under 20X microscope objective.

The diameter of the core, through which light travels, remained $5\mu\text{m}$, and the optical performance was unchanged. This etching was performed to increase the pressure on the epoxy during probe preparation. The pressure is given by

$$\begin{aligned} \text{Pressure (P)} &= \text{Force/ Area} \\ &= F/ A \end{aligned} \tag{12}$$

By reducing the area, more pressure can be applied with the same force resulting in a thinner layer of epoxy at the end of this fiber. A wooden structure with screw and spring was used to apply an equal amount of force on the fiber to reduce the thickness of the epoxy (Figure 5.9).

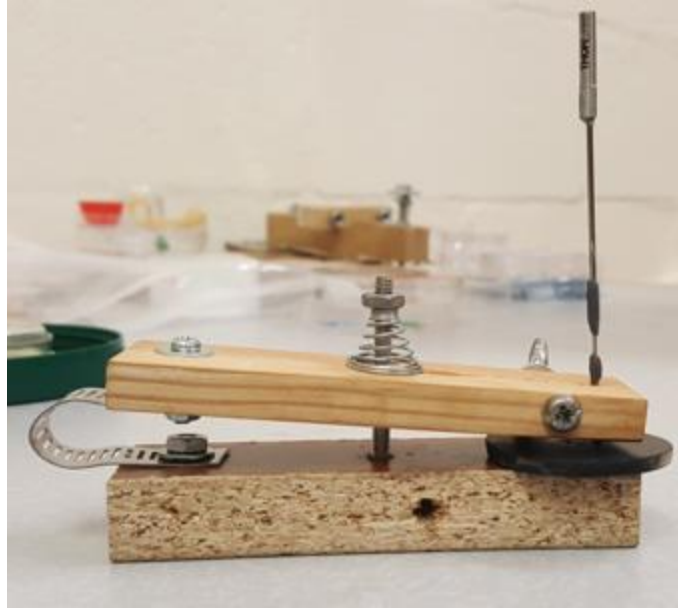


Figure 5.9. Wooden structure with spring used for applying pressure to thin the epoxy at the end of the fiber.

5.4 Connecting Probe to the End of an Articulate Arm

Laser light left the spectrometer as a parallel beam, whose width was adjusted by a Galilean telescope. The fiber was coupled by the GRIN lens to the spectrometer through a mirrored arm. Joints in the arm, which was previously reported by J. Kim et. al, [33, 41] permit the needle to be placed at any angle and anywhere within a working volume of about 1 cubic foot. A total of seven mirrors (2 external mirrors to guide the laser beam to enter the arm and 5 internal mirrors in the arm) were used in the system. All 5 internal mirrors were mounted at 45° angles. Therefore, whenever any joint rotates, the laser beam reflects at 90° , and travels to the end of the arm.

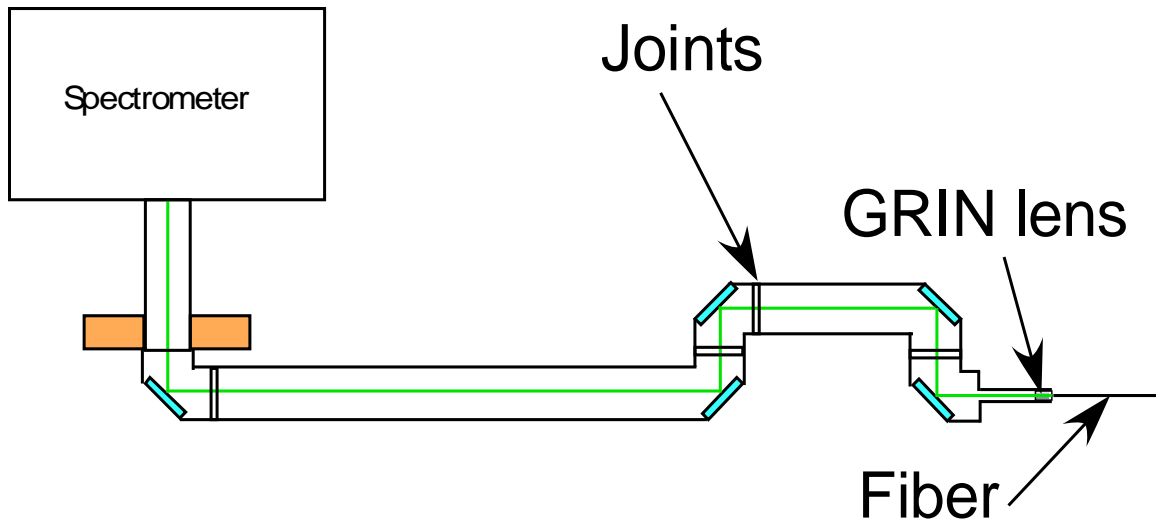


Figure 5.10. Schematic diagram of the articulate arm connected to fiber probe and Raman spectrometer [55]

The probe is connected to the articulate arm by a tilting table to direct the beam at the correct angle to the GRIN lens. The laser beam travels as a parallel beam to the GRIN lens, where it is coupled to a numerical aperture = 0.12 optical fiber.

Figure 5.10 is a schematic diagram of the articulated arm with probe, and Figure 5.11 is a photograph of the set up consisting of Raman Spectrometer, Galilean telescope, mirror coupled articulate arm, tilting table, and SERS probe with GRIN lens.

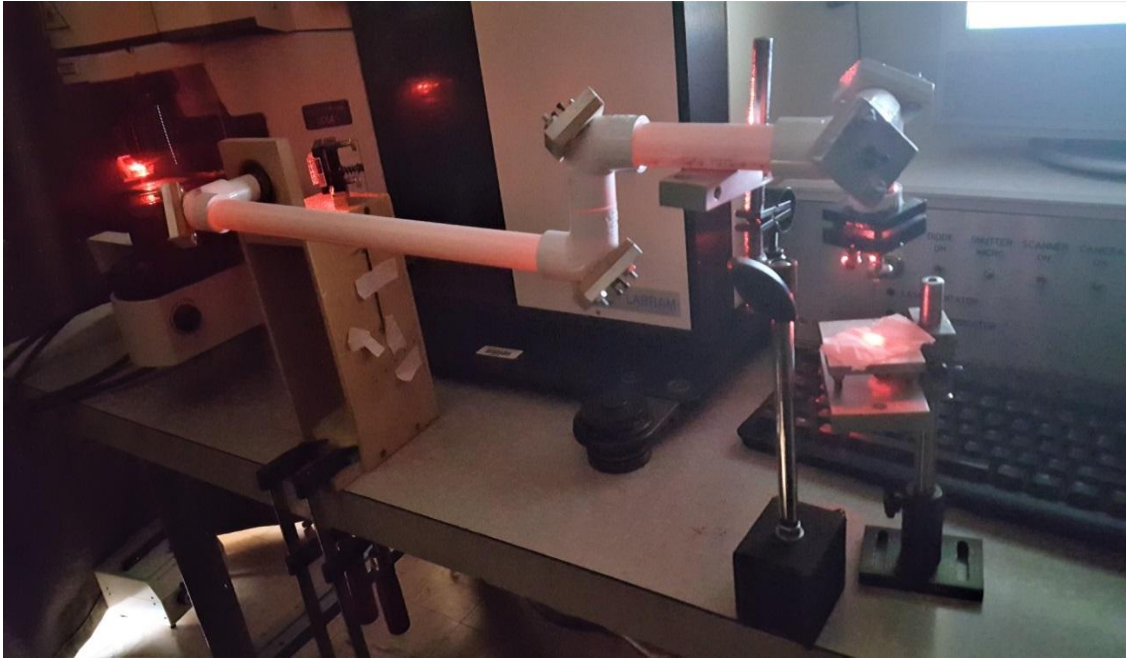


Figure 5.11. Photograph of the system

A Raman spectrum was obtained with the needle probe in air. There is a prominent peak at 800 cm^{-1} . This was generated internally by the epoxy in the probe and its run to run reproducibility, about $\pm 10\%$, is a useful check and helps to calibrate the system gain. A corresponding Raman spectrum was obtained by the needle probe in DI water. The spectra are similar in shape but slightly different in intensity (Figure 5.12). The water may reduce the coupling of the Raman signal from the epoxy back to the fiber.

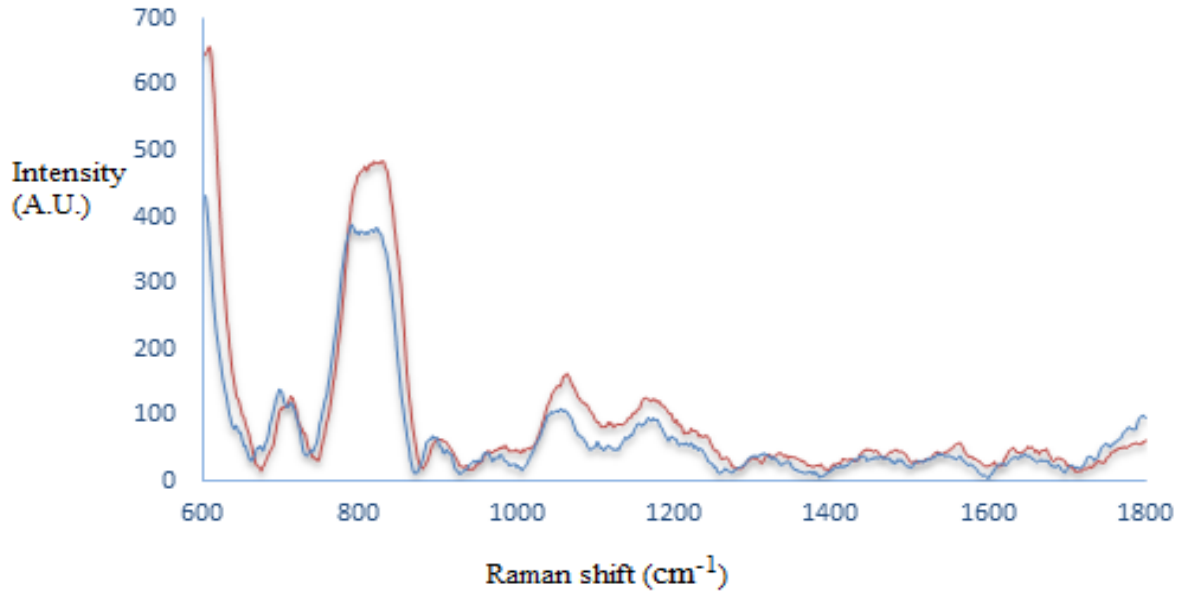


Figure 5.12 Raman spectrum obtained from needle in air and DI water. The red spectrum is from the needle probe in air and the blue spectrum is from the needle probe in DI water

5.5 Conclusions

This chapter described the fabrication of the single fiber SERS needle probe, and how a flexible pre-built articulate arm [33, 41] is connected to the probe for remote operations.

The air path connected probe not only increased the flexibility of the positioning of the specimen but also overcame problems in previously reported probes by other groups using multiple optical fibers.

CHAPTER 6: DETECTION USING THE PROBE SET UP

6.1 Introduction

Cancer is a worldwide problem, which causes a huge number of deaths. [56- 58] A biopsy is one of the common ways of detecting cancer, where experts examine the tissues or cells under a microscope. [59-61] By applying this research an abnormality of a tissue can be detected without taking it outside the body, which reduces the post procedural risk of a biopsy. [62] In addition, multiple detections are possible for a single insertion, in situations where multiple biopsies are not practical.

Raman signals were obtained with the needle probe and articulate arm described here from doped gelatin blocks and within organs obtained from freshly sacrificed mice.

6.2 Detection of Gelatin using Different Concentrations of Rhodamine 6G Solutions

Raman signals were obtained by inserting the probe into blocks of gelatin containing Rhodamine 6G dyes (Figure 6.1 and Figure 6.2).

Some sections of this chapter in its current form are published in a journal article. It is reproduced with changes from [Srismrita Basu, Hsuan-Chao Hou, Debsmita Biswas, Subhodip Maulik, Theda Daniels-Race, Mandi Lopez, Michael Mathis, and Martin Feldman, "A needle probe to detect surface enhanced Raman scattering (SERS) within solid specimen", *Review of Scientific Instruments*, 88(2), 2017] with the permission of AIP Publishing (Appendix A)

Some sections of this chapter in its current form are published in a journal article. It is reproduced with changes from [Srismrita Basu, Hsuan-Chao H,ou, Debsmita Biswas, Theda Daniels-Race, Mandi Lopez, Michael Mathis, and Martin Feldman, "A Single Fiber Surface Enhanced Raman Scattering (SERS) Probe" *Journal of Vacuum Science & Technology B, Nanotechnology and Microelectronics: Materials, Processing, Measurement, and Phenomena*, 25(6), 2017] with the permission of JVSTB Publishing (Appendix B)



Figure 6.1. Photograph of Probe at end of articulated arm inserted in Gelatin block

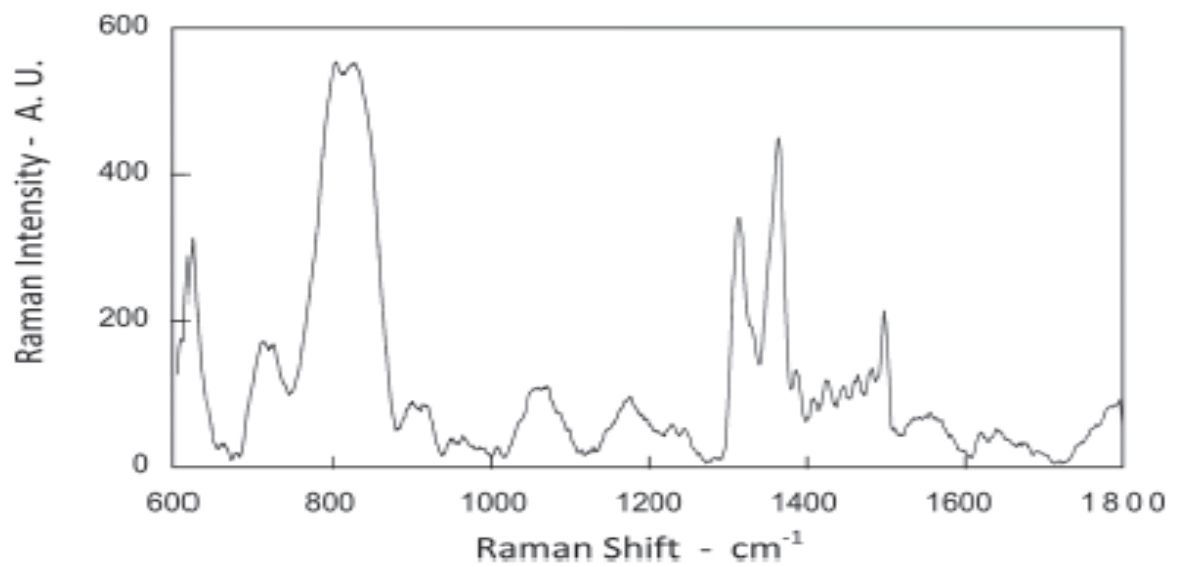


Figure 6.2. Raman spectrum of Gelatin made with 1mM R6G solution using the needle probe connected to the articulate arm [46]

SERS results (Figure 6.3. and Table 6.1) from a needle inserted into gelatin blocks made with different concentrations of R6G solutions showed a signal variation of less than a factor of 10, over a range of 1000 in concentration. Round trip losses in the mirrors reduced the signal strength by a factor of 2. After correcting for the loss, the signal strength was comparable to the conventional operation of the spectrometer with a microscope objective with the same NA (0.12). The result demonstrates the usefulness of a single fiber half millimeter diameter needle probe in solid specimen.

Table 6.1. Raman intensity for Gelatin prepared by different concentrations of Rhodamine 6G solutions measured by needle probe connected with the articulate arm to the Raman spectrometer.

Concentration of R6G in Gelatin	Raman Intensity (A.U.)
DI water	0
1 μM	70
10 μM	140
100 μM	232
1000 μM	460

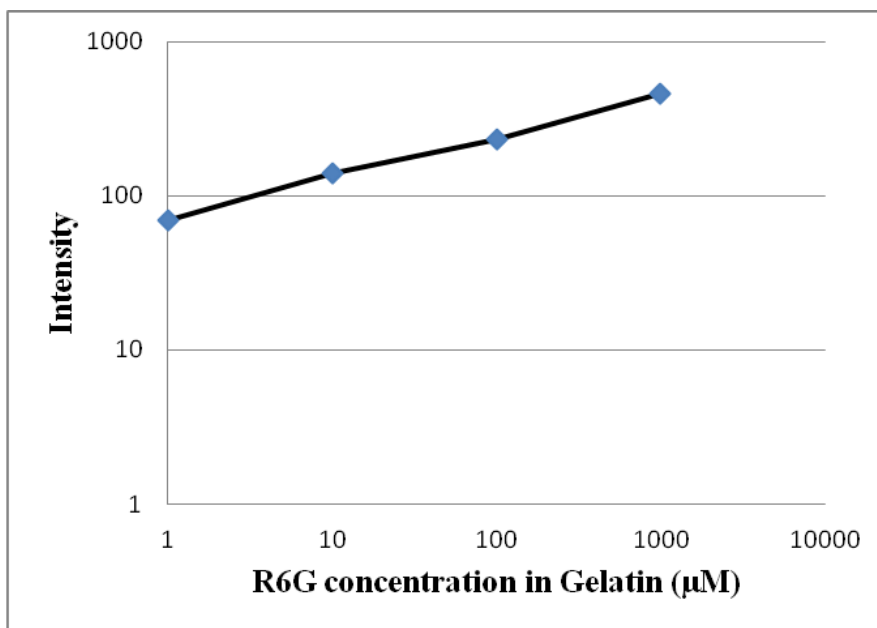


Figure 6.3. Intensity vs. R6G concentration in gelatin [46]

6.3 Detection of Various Mouse Tissues

Raman spectra from mouse tissues were also obtained by inserting the probe into organs removed from mice. The results are shown below in Figure 6.4.

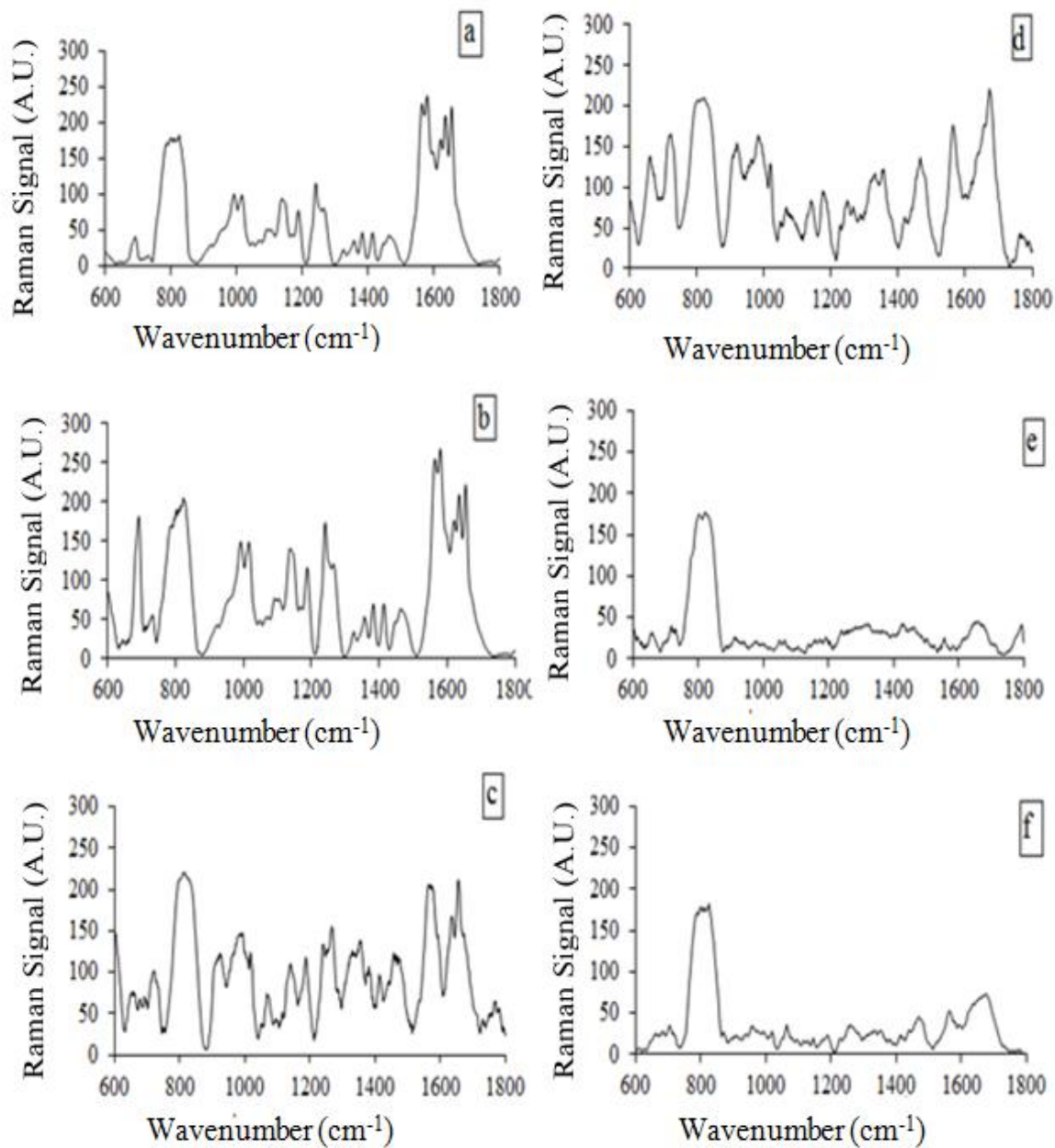


Figure 6.4. Raman spectra for (a) Lungs, (b) Kidney, (c) Heart, (d) Liver, (e) Skin, and (f) Muscle from freshly removed organs of mice using the needle probe connected with the Raman spectrometer through the articulate arm. [55]

Multiple measurements of tissue were made by inserting the needle in different locations and multiple times at the same position as well to verify the data. The intensity varied by $\pm 50\%$, but the shape of the spectra remained the same to within $\pm 10\%$.

The variations arose from the granularity of the biological samples; individual cells were several microns apart causing variations in how close some approached the rough gold. However, even though the gain varied from run to run, the shapes of the spectra were consistent.

6.4 Detection of Cancerous Tumor of a Mouse

Raman signals were obtained by inserting needle probes into a cancerous colon tumor and a healthy colon obtained from freshly sacrificed mice. Multiple measurements were made by inserting the probe into different sections of the colon for both healthy and cancerous colons. Figure 6.5 and Figure 6.6 are photographs of the needle probe in a healthy colon and cancerous colon respectively.

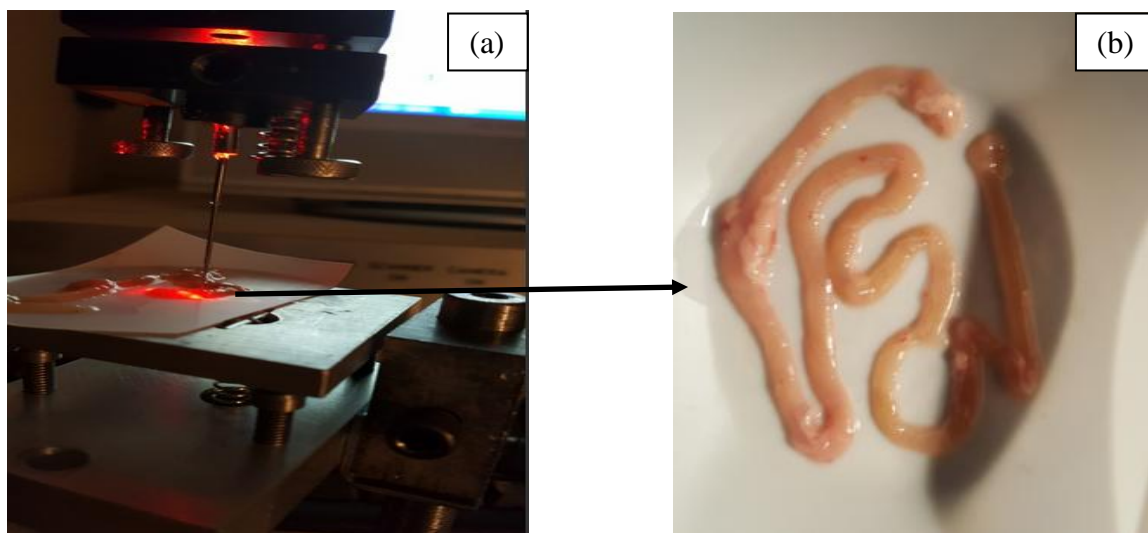


Figure 6.5. Photograph of (a) needle probe in healthy colon, (b) healthy colon taken out from a freshly sacrificed mouse

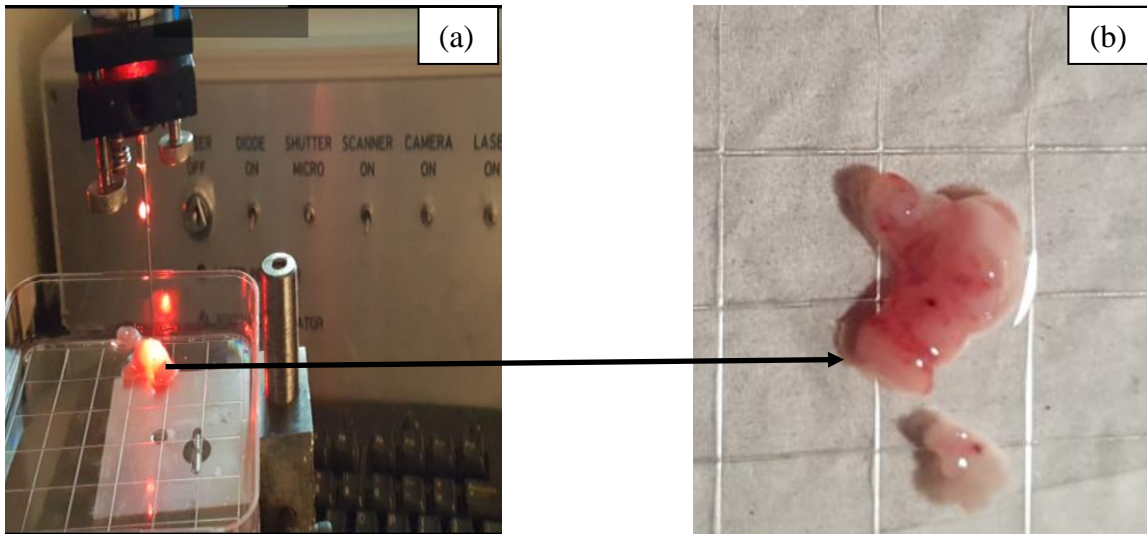


Figure 6.6. Photograph of (a) needle probe in cancerous tumor, (b) cancerous tumor taken out from a freshly sacrificed mouse

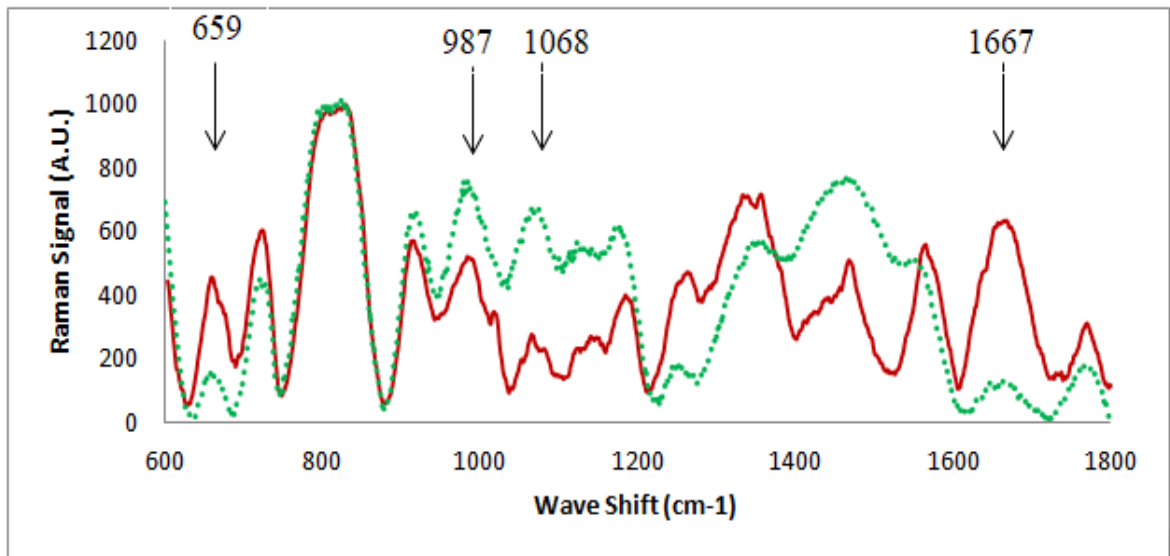


Figure 6.7. Raman spectra obtained by a needle probe into mouse colons. The dotted curve is for a healthy colon, the solid curve for a cancerous colon tumor [55]

The dotted green curve in Figure 6.7 is the average of 10 Raman spectra taken at different sites in the colon of a healthy mouse; the solid red curve is the average of 4 Raman spectra from a cancerous tumor in a mouse colon. The prominent peak at 800 cm^{-1} arises internally in the

probe due to epoxy and its run to run reproducibility, about $\pm 10\%$, is a useful check and helps to calibrate the system gain. This is an additional advantage over two fiber systems using separately implanted metallic nanoparticles; abnormalities may be identified by signal strength differences between sites, which is not possible with uncertain concentrations of the inserted nanoparticles.

The average standard deviation at each point was about 50%, much larger than for the epoxy peak or for runs taken in solutions of Rhodamine dye. It is believed the variations arose from the granularity of the biological samples; individual cells were several microns apart causing variations in how close some approached the rough gold. However, even though the gain varied from run to run, the shapes of the spectra were consistent and there were strong correlations between different parts of the spectrum. Consequently, the ratio between any two spectral lines in the same run was much more reproducible, with a standard deviation of 5 to 10%, even though the run to run reproducibility was around 50%. This property was used to distinguish between spectra.

The spectra of healthy and cancerous colons in Figure 6.7 are significantly different. In four places in the spectra the differences are particularly large. A quantitative measure of the differences was obtained by selecting spectral lines from these places. In two of these lines (labeled ν_1) the cancerous Raman signal was greater than the healthy one, and in two of them (labeled ν_2) it was smaller (Table 6.2). All four ratios, ν_1/ν_2 , between each ν_1 spectral line and each ν_2 spectral line were calculated for each run. The average ratio of several runs and its standard deviation were computed for each ν_1/ν_2 . The ratios are different for the healthy tissue and the tumor.

In each of the four cases in Table 6.2, the difference in the ratios is ≥ 4.8 standard deviations. Statistically, a difference of 4.8 standard deviations occurs less than 1 time in 1,000,000. Larger standard deviations are even less likely. So, it is mathematically certain that the cancerous tumor and the healthy tissue are different.

Table 6.2. Ratios of the intensities of Raman spectral lines, v_1 to v_2 , for cancerous tumors and healthy mouse colon cells. In all four cases, the ratios are much larger for tumors than for healthy colons, with differences of many standard deviations [55]

$v_1(\text{cm}^{-1})$		$v_2(\text{cm}^{-1})$	
		987	1068
659	Tumor	0.94±0.13	1.82±0.13
	Healthy	0.22±0.08	0.26±0.16
	Difference	0.72±0.15	1.56±0.21
	St. Dev.	4.8	7.4
1667	Tumor	1.25±0.15	2.520±0.08
	Healthy	0.18±0.06	0.18±0.08
	Difference	1.07±0.06	2.32±0.12
	St. Dev	6.7	19.3

6.5 Conclusions

After correcting for known losses in the light path, the signal was comparable to that obtained from the specimen viewed directly by the spectrometer. The flexibility of positioning obtained with the articulate arm combined with the strong signal makes these probes attractive for clinical applications.

With the thin needle probes multiple sites can be examined at a time. For example, in the prostate where many small, closely spaced areas need to be examined, this process will be extremely helpful. In addition, there is no need to insert and/or remove nanoparticles near suspected cancer sites. The sensitivity is constant because the same rough surface, attached to the probe, is always used. Consequently, abnormalities may be identified by signal strength differences between sites, which are not possible with uncertain concentrations of inserted nanoparticles. Moreover, the results are available immediately, without the need for return patient visits.

In conclusion, a single fiber SERS probe is a minimally invasive method to obtain robust diagnostic Raman spectra.

CHAPTER 7: SURFACE ENHANCED RAMAN SPECTROSCOPIC SUBSTRATE UTILIZING GOLD NANOPARTICLES ON CARBON NANOTUBES

7.1 Introduction

This chapter reports a state of the art low cost technique to fabricate Surface Enhanced Raman Spectroscopy (SERS) substrates. A Gold (Au) nano-metallic structure for surface enhancement is created by depositing Au nanoparticles on a Multi-wall Carbon Nanotube (MWCNT) layer pre-deposited on an etched Aluminum foil. Low cost and simple methods are used to deposit the nanotubes. Significant enhancements in signal strength have been observed in both *in vitro* and *ex vivo* like measurements.

The enhancement for Surface Enhanced Raman Scattering (SERS) substrates occurs when the nano-metallic structures contain features that are smaller than the wavelength of the incident monochromatic light ^[63]. The enhancement is highly surface geometry dependent. The current technologies involved in fabrication of SERS substrates are mostly expensive, labor intensive and time consuming ^[64- 68].

7.1.1: Carbon Nanotubes (CNTs)

Although CNTs were first discovered in 1952 by Radushkevich and Lukyanovich, they received much more attention when they were rediscovered by Sumio Iijima in 1991^[69-70]. CNTs are basically single or multiple roll of graphene sheets ^[71].

Some sections of this chapter in its current form is published in a journal article. It is reproduced with changes from [Srismrita Basu, Subhodip Maulik , Hsuan-Chao Hou, , Theda Daniels-Race, and Martin Feldman, "Surface Enhanced Raman Spectroscopic Substrate Utilizing Gold Nanoparticles on Carbon Nanotubes", *Journal of Applied Physics*, 122(17), 2017] with the permission of AIP Publishing (Appendix C)

When a 2-D graphene sheet is rolled once into a nanometer-diameter single tube or cylinder it forms a single walled carbon nanotube (SWCNT), and when the sheet is rolled multiple times it forms a multi walled carbon nano tube (MWCNT). CNTs have a wide range of applications due to their unique electrical, mechanical and thermal properties. The electrical conductivity of the CNTs is determined by the helicity of the CNT structure. The variation by which the graphene sheets are rolled up explained the helicity of the tubes represented by a chiral vector ($C = na_1 + ma_2$). The numbers n and m represents pair of integers and a_1 and a_2 represent unit vectors along the direction of the crystal lattice of the graphene sheet. If $m = 0$ or $n = 0$, the CNTs are called Zigzag nanotubes, and if $m = n$, the CNTs are called armchair nanotubes. Otherwise they are known as chiral. [76] Depending on its chirality a CNT can behave as a metal (when it has armchair structure) or as a semiconductor (when it has chiral structure). Under tension it is the strongest material in the world due to its strong carbon-carbon covalent bond. In addition, CNTs are light weight, and have a high elastic modulus, super conductivity (below 20°K), and high thermal conductivity.^[72-75]

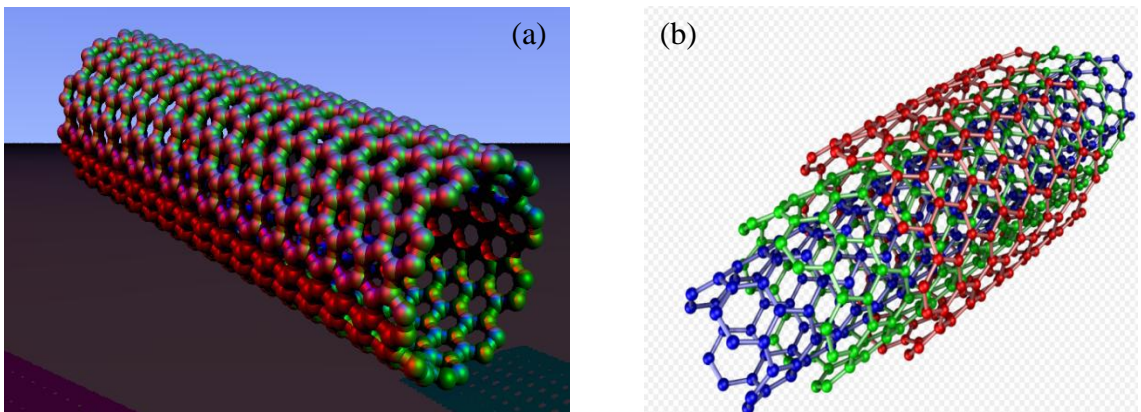


Figure 7.1. (a) Single walled carbon nanotube (SWCNT), (b) Multi walled carbon nanotube (MWCNT) (Triple layer). [76]

Instead of expensive and laborious Chemical Vapor Deposition (CVD) and/or lithographic steps we have developed a unique gold coated MWCNT SERS technology that is cost efficient and fast. In addition our SERS substrates are far more rugged than existing substrates, an important consideration for many SERS applications. Au was chosen for this work because it is non-toxic, has a high melting point, does not oxidize, and has high etching selectivity. Household aluminum foil is used as a sacrificial substrate. Al foil was chosen as it is readily available and is easily etched in Potassium Hydroxide (KOH).

7.2 Experimental Procedure

7.2.1: Substrate Preparation

The aluminum foil was first cleaned by the process described in section 4.4.1. Previous work showed ^[11, 13, 31] maximum SERS was obtained after stirring assisted etching of the back side of the aluminum foil. Accordingly, the foil was etched for 1 minute at room temperature in 30% Potassium hydroxide (KOH), followed by a DI water rinse and nitrogen gas drying. Approximately 1 μ m thickness of aluminum was removed by etching.

7.2.2: Multi wall Carbon Nanotube Preparation

Two batches of MWCNT suspension were prepared. One batch of MWCNT suspension was prepared with Isopropyl alcohol (IPA) and Sodium Dodecyl Sulfonate (SDS) as described by Maulik et.al. ^[77-78] In this method 40 mgs of SDBS was mixed with 200mL of IPA. Then this mixture was ultra-sonicated for 10minutes. 100mg of MWCNTs were added to this SDBS and IPA based solution and again ultra-sonicated for 20minutes using a tip sonicator while putting the beaker containing the MWCNT suspension in ice bath.

A second batch of MWCNT suspension was prepared using the Acid Refluxing method described by Sarkar et.al^[79- 83]. In this method, 100mg of as-purchased MWCNT powder was mixed with 30mL of concentrated sulfuric acid 10mL of concentrated nitric acid. This mixture was stirred for 15minutes and then heated at 70⁰C temperature for 20 minutes. It was cooled by putting the beaker containing the solution in an ice bath. Then, this solution was washed with deionized water using a Buchner funnel set up and a filter paper until the solution achieved a pH level of 7. Finally, the MWCNTs were mixed with 50mL IPA, and sonicated to get the MWCNT suspension.

7.2.3: Deposition of MWCNT Suspension on Substrate

MWCNTs were deposited on aluminum foil. Instead of the more common, labor intense and costly, Chemical Vapor deposition (CVD)^[84- 87] two alternative MWCNT deposition techniques were used: 1) Casting droplets of a suspension of MWCNT and 2) Voltage controlled spraying of the MWCNT suspension^[77, 78, 88]. Both methods are fast and inexpensive. Both batches were deposited on the back side of the stirred-etched aluminum foil, using both drop casting and voltage controlled spraying (Table 7.1). For drop casting multiple drops of MWCNT suspension were dripped on the Al foil. Both acid refluxed MWCNT solution and surfactant assisted MWCNTs suspensions were used to prepare two separate set of samples.

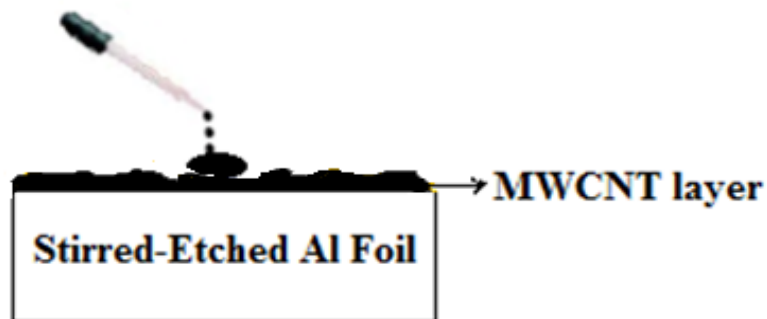


Figure 7.2. Drop casting method. Gold was sputtered after the MWCNT were deposited.

For voltage controlled spraying, we followed the method developed by Maulik et.al^[77, 78, 88], where a 70nm thick MWCNT layer was developed by spraying for 40seconds with a 7 KVolt DC voltage. The Al foil was mounted on a rotating disc to get a uniform thickness of the MWCNT layer.

7.2.4: Au Sputtering on MWCNT Coated Etched-Stirred Al foil

20nm of Au was sputtered on the deposited MWCNT, creating a nano-metallic structure of nano-islands of gold on the MWCNTs. A circular magnetron sputtering chamber (Oxford Plasma Lab System 400 Sputtering System) was used. The gold layer appeared visually uniform and was transparent.

MWCNT prepared by IPA and SDS and deposited on the back side of etched-stirred aluminum foil by the voltage controlled deposition method had the maximum enhancement and this substrate was chosen for gold deposition. Scanning Electron Microscope images of MWCNTs on stirred-etched Aluminum foil before and after 20nm sputtered Au are shown in Figure 7.3. The MWCNT layer formed a bird nest/ spaghetti like structure, where CNTs are

placed horizontally very close to each other. When gold is sputtered on them it creates closely packed nano-structures which are ideal for enhancement.

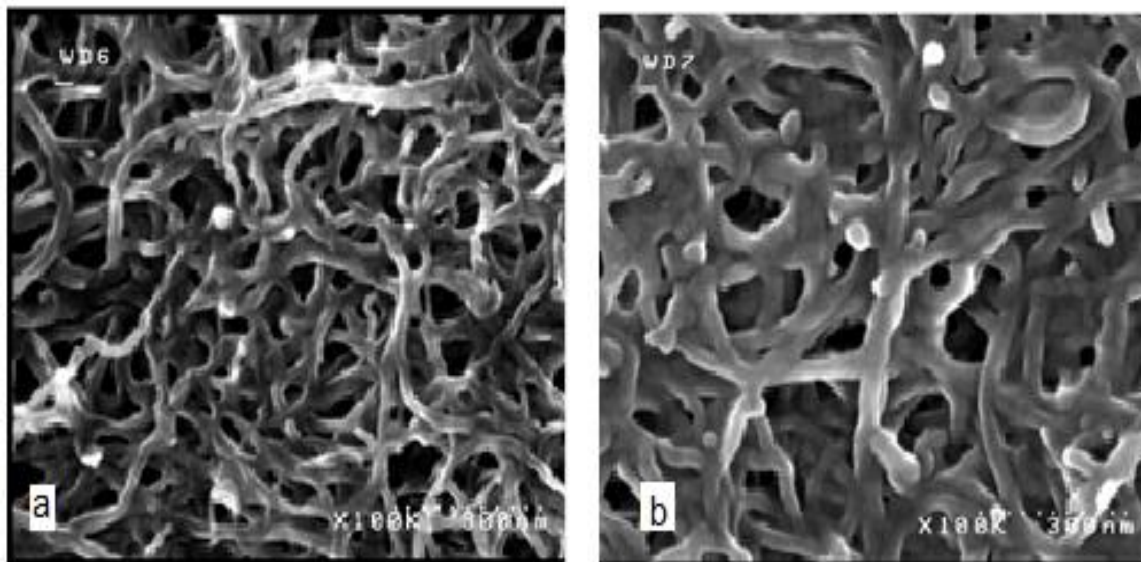


Figure 7.3. (a) SEM image of CNT deposited on stirred-etched aluminum foil (b) SEM image of 20nm sputtered gold on CNT deposited on stirred-etched aluminum foil. Both images were taken with 100,000 X magnification. [89]

7.2.5: Preparation of Rhodium 6G Solution

Solutions of Rhodamine 6G (R6G) were used as specimen for SERS. The powdered R6G was dissolved in de-ionized water at 50°C temperature by stirring the solution for 3-4 hours. Solutions were prepared varying in concentration from 1pM to 1mM in steps of 10.

7.3 Results

Drops of the R6G solution were placed on microscope slides under cover slips (Figure 7.4). The cover slips delayed the evaporation of the R6G solution and created a flat optical surface. The laser light from the Raman spectrometer was focused on the substrate through the

solution, and the measurement was done immediately after putting a single drop of R6G solution on the SERS substrate.

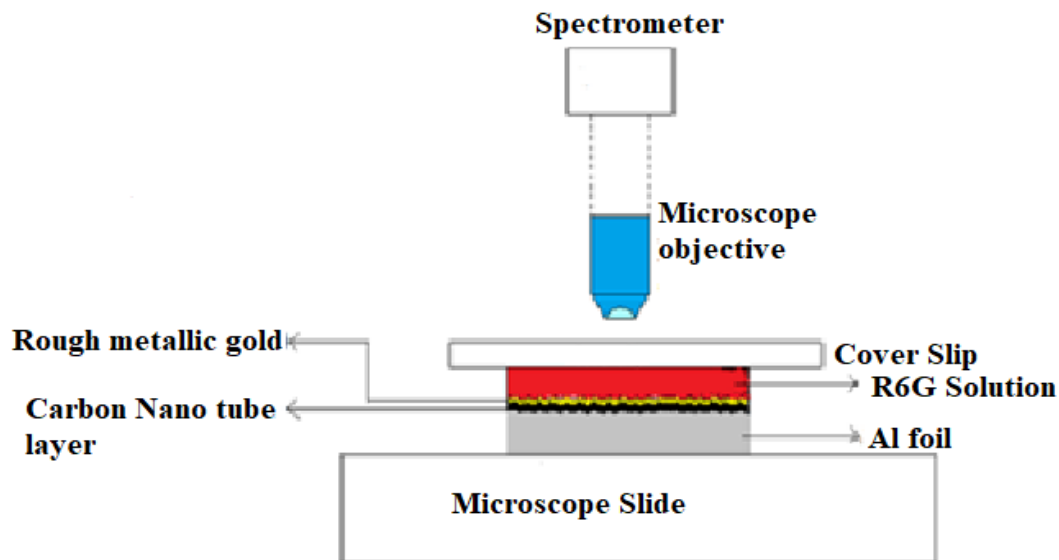


Figure 7.4. *In vitro* arrangement for SERS [89]

A SERS spectrum obtained at a concentration of 1mM (Figure 7.5) shows the principle peaks of R6G at 610, 771, 1180, 1310, 1360, 1504, 1647 cm^{-1} [90]. The signal arising from the DI water on gold coated MWCNT in IPA on the etched-stirred Al foil is shown for comparison (Figure 7.6). This spectrum does not contain any MWCNT peak or any specific peak from the SERS substrate. The relative signal strengths at 1360 cm^{-1} are given in Table 7.1 for different methods of MWCNT preparation.

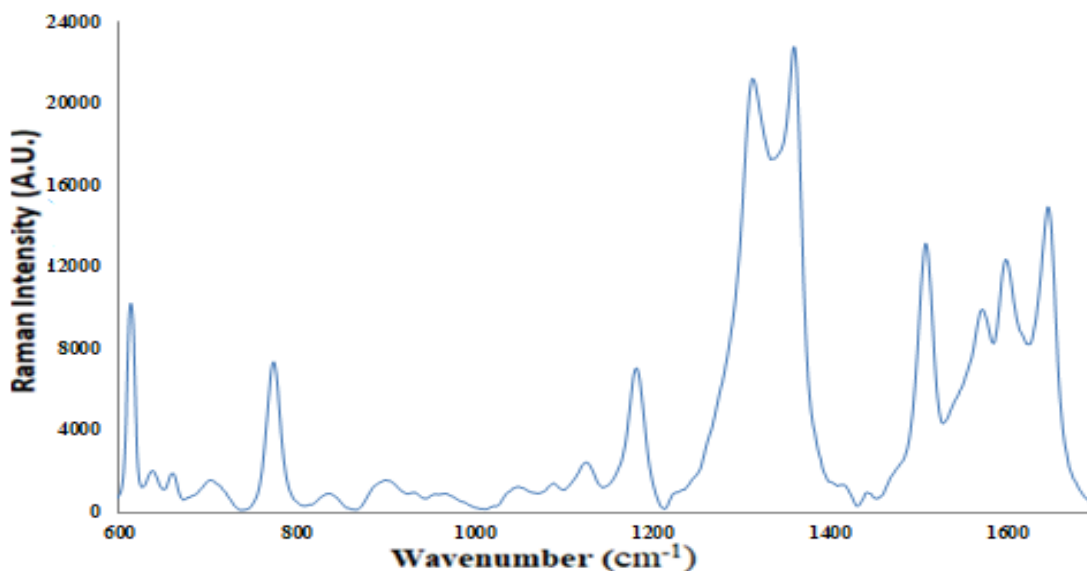


Figure 7.5. Raman signal (with a microscope objective of NA=0.55) 1mM R6G solution on gold covered MWCNT on etched-stirred Aluminum foil [89]

Table 7.1. Raman intensities of 1mM R6G solution for different types of substrates (CNT layer on back side of etched-stirred aluminum foil)

	Acid Reflux	IPA and SDS
Drop Casting	814	5107
Voltage Controlled	1505	5428

SERS signals were obtained for R6G concentrations from 1nM to 1mM. Over a factor of 10^6 change in the concentration of R6G the Raman signals changed by a factor of 650 (Figure 7.6). All the data were averaged over 15 measurements taken after putting a single drop of R6G solution on the SERS substrate and were reproducible to about $\pm 7\%$.

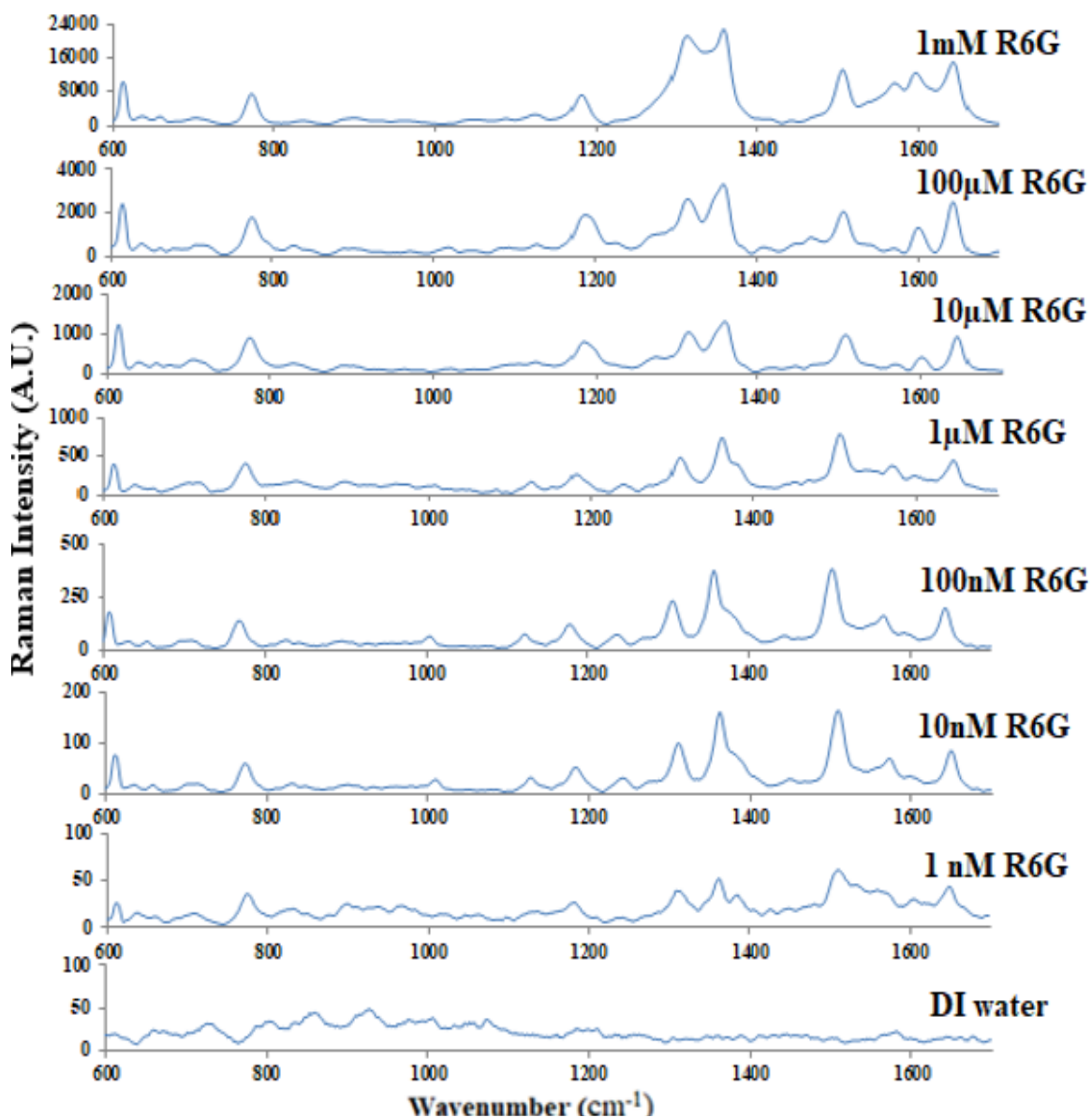


Figure 7.6. Raman signals of R6G solutions (using 50x microscope objective) for gold on MWCNT on the back side of etched-stirred Aluminum foil as a function of the wavenumber, Concentration of R6G vary from 1nM to 1mM by a factor of 10. [89]

The substrate was epoxied to a microscope slide with the gold layer facing the epoxy. The Al foil was etched and the MWCNT was removed by ashing. Only a thin layer of rough gold remained epoxied to the slide. This produced a much stronger bond between the gold nano particles and the glass than directly deposited gold.⁵¹ In addition the higher roughness of the

resulting gold nanostructure greatly increased the Raman signal intensity. The strong bond to the glass permits forceful contact with solid specimen. In addition it is not necessary for the specimen to be transparent as in Figure 7.4, as the signal is obtained by viewing through the gold in contact with the specimen (Figure 7.7).

With the additional processing signals were detected from concentrations of R6G as low as 1pM. This indicates a much larger enhancement of the signal after ashing (Figure 7.8 and Figure 7.9).

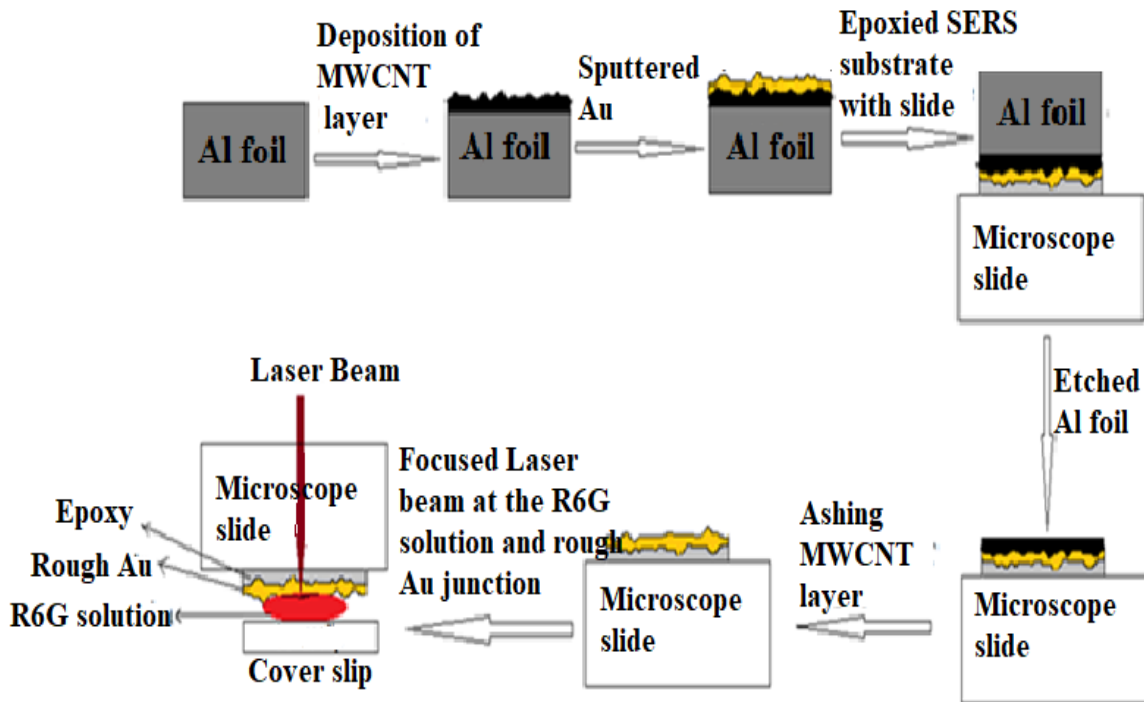


Figure 7.7. Process of sample preparation and measurement for *ex vivo* like method [89]

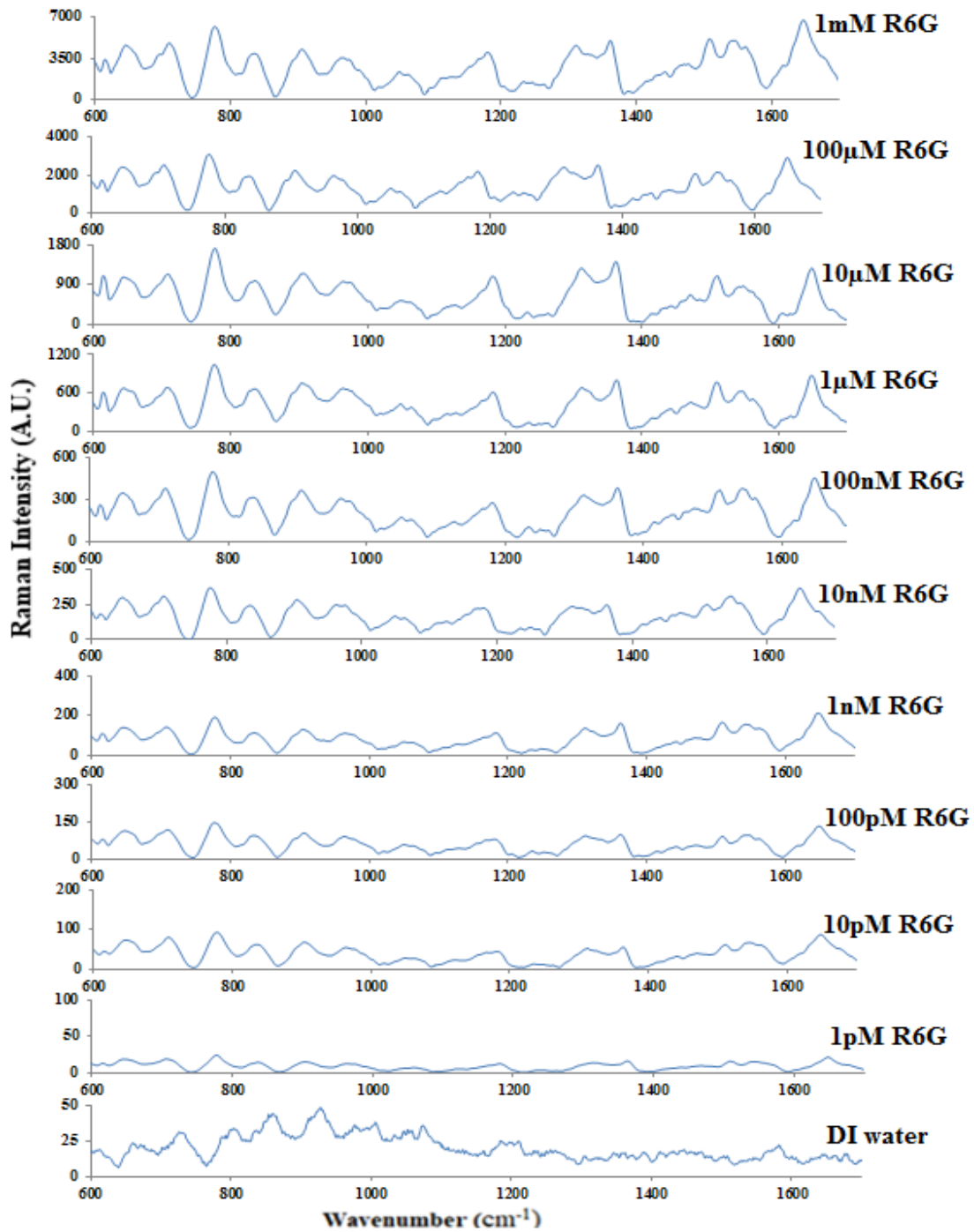


Figure 7.8. Raman signals of R6G solutions (using microscope objective of NA= 0.55) for viewing through gold on the back side of etched-stirred Aluminum foil, after ashed the MWCNT layer, as a function of the wavenumber, Concentration of R6G vary from 1nM to 1mM by a factor of 10. [89]

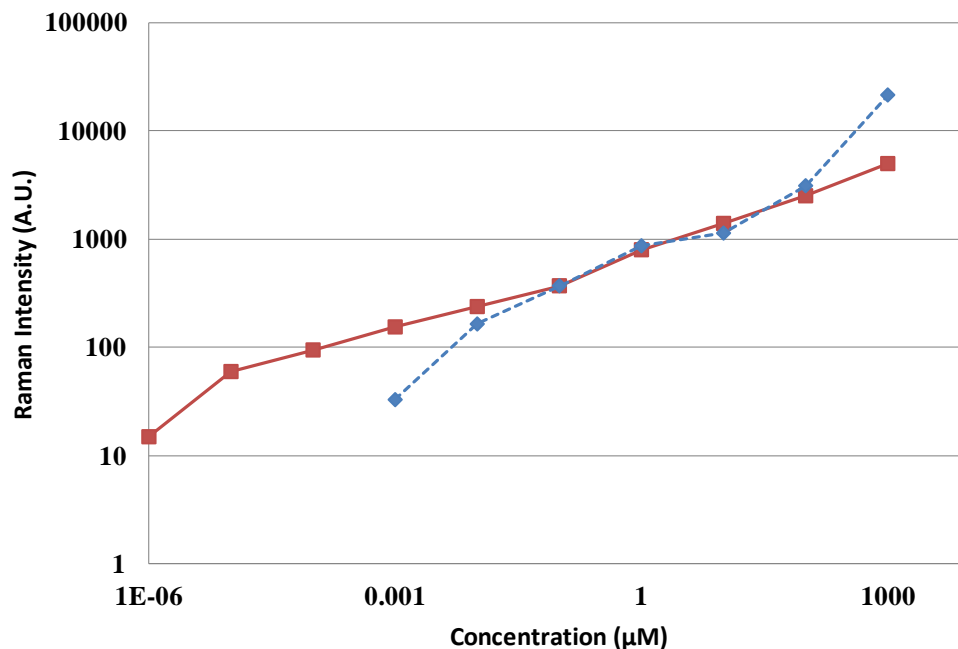


Figure 7.9. Raman signals (using 50x microscope objective) for viewing through epoxy and gold after ashing as a function of the concentration of R6G solutions (Red solid curve), and Raman signals (using 50x microscope objective) for gold on MWCNT on the back side of etched-stirred Aluminum foil as a function of the concentration of R6G solutions (Blue dotted curve). [89]

A SERS probe is developed using this SERS substrate following the same process described in the Chapter 5 (Figure 5.7). The enhanced Raman spectrum for 1mM R6G solution in gelatin is given below (Figure 7.10). The sensitivity of this probe is higher than the probe developed with sputtered gold on the back side of the stirred-etched Al foil.

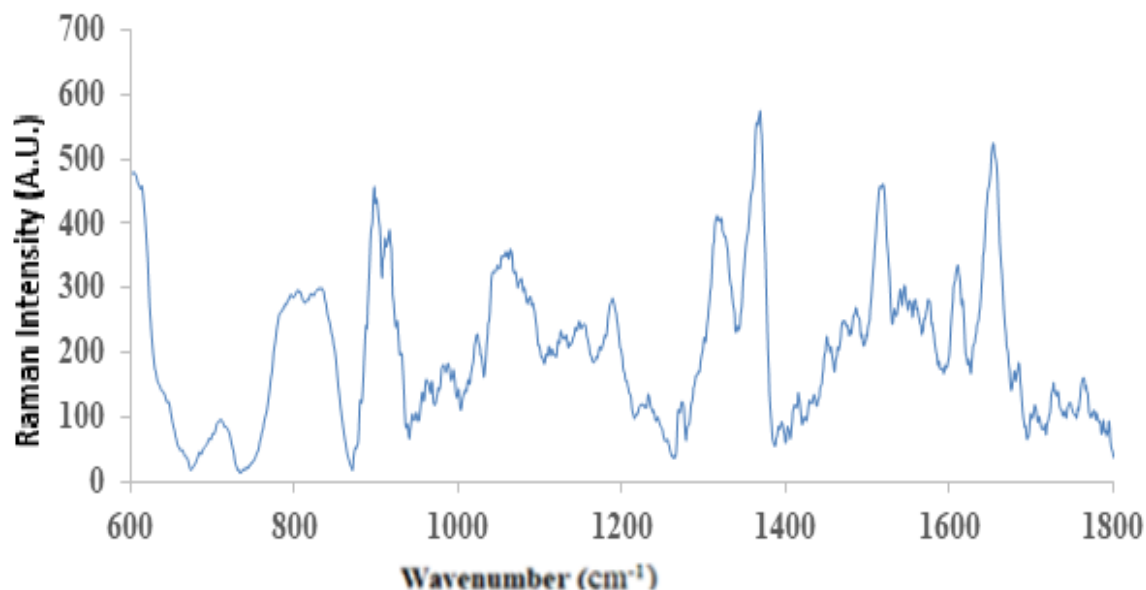


Figure 7.10 Raman signal of 1mM R6G solution in gelatin using optical fiber probe with Au coated MWCNT on Al foil

7.4 Conclusion

This chapter reports the preparation of a Surface Enhanced Raman Spectroscopic substrate using Carbon nanotubes and Gold without costly Chemical Vapor Deposition and lithographic steps. The signal from gold plated aluminum foil is increased by stirring assisted etching, carbon nanotube deposition, and a subsequent etch to remove the nanotubes (Table 7.2).

This MWCNT assisted SERS substrate is used for the development of SERS probe for clinical applications. This newly developed SERS probe is much sensitive than the probe described in chapter 5. The bird nest structure of MWCNT layer with sputtered Au on is the reason behind this enhancement.

Table 7.2. Signals from a 1mM suspension of R6G on different substrates

Types of substrate	Intensity
Non-etched Al foil (Back side)	232
Stirred etched Al foil (Back side)	282
MWCNT on stirred etched al foil (Back side)	5428
Au on MWCNT on stirred etched Al foil (Back side)	21500

CHAPTER 8: SURFACE ENHANCED RAMAN SCATTERING SUBSTRATE USING GOLD NANO-PARTICLES ON THINNED SILICON WAFER

8.1 Introduction

Gold nanoparticles were sputtered on the smooth side of a polished silicon (Si) wafer to create a Surface Enhanced Raman Scattering (SERS) substrate. The specification of this silicon wafer is given below (Table 8.1). In order to use this SERS substrate in future for the fabrication of a clinical probe it was thinned by one-sided etching.



Figure 8.1. Photograph of the $\langle 1-0-0 \rangle$ Silicon wafer

Table 8.1 Specification of the Silicon wafer

Type	N
Thickness	400 μ m
Diameter	3"
Orientation	$\langle 1-0-0 \rangle$

8.2 Substrate Preparation

8.2.1: Substrate Cleaning

The aluminum foil was first cleaned following the process described in section 4.4.1.

8.2.2: One Sided Etching of the Silicon Wafer

The in-built nano structure on the smooth/polished side of the Si wafer was intended to be used by sputtering Au on it. But, due to the large thickness of the wafer it was difficult to attach it at the end of an optical fiber.

1. The larger the thickness the larger the weight of the wafer. So, a very strong epoxy is needed to hold it at the end of the fiber.
2. Large thickness increases the etching time as well. In this work an alternate method of nano structure fabrication at the end of the probe is developed and used, where the SERS substrate is attached with epoxy at the end of the fiber and then etched. After etching the nano structure is at the end of the fiber attached by the epoxy.

The first problem can be solved by using a strong epoxy. “AB” epoxy (Harbor Freight Tools brand, Camarillo, California) is transparent, strong, and become solidifies in 5 minutes. Although several other epoxies were tried “AB” epoxy produced the best result (Table 8.2). In order to solve the second problem, the wafer was thinned by etching the back side. But, after a certain thickness the wafer will becomes so fragile that it is impossible to attach it at the end of the fiber.

Table 8.2 Comparison of different type of epoxies

Epoxy	Advantage	Disadvantage
2 TON epoxy Devcon home (Danvers, Massachusetts)	Transparent	Not very strong, Held the wafer for 2 hours at the end of the fiber at 50 ⁰ C in 30% KOH
Industrial Glue E6000- Clear (Eugene, Oregon)	Transparent	Held the wafer for 3.5 hours at the end of the fiber at 50 ⁰ C in 30% KOH
Gorilla Glue The Gorilla glue company (Sharonville, Ohio)		Not transparent, Held the wafer for 2.5 hours at the end of the fiber at 50 ⁰ C in 30% KOH
“AB” epoxy Harbor Freight Tools brand (Camarillo, California)	Transparent. Very strong. Held the wafer for 5 hours at the end of the fiber at 50 ⁰ C in 30% KOH	

A set up was made for wet etching the wafer (Figure 8.2). The specifications of this set up are given in Table 8.3.

Table 8.3 Specifications of the set up

Inside diameter of the small tube	0.6''
Height of the small tube	0.71''
Inside diameter of the big tube	2.6''
Height of the big tube	1.5''
Power of the bulb	75watt
Distance between KOH level to bulb	1.8''

In order to etch the wafer from one side to a thickness of 120 μ m first a small Teflon tube was used (shown in Figure 8.2 (a)) to etch a small section of the wafer (Figure 8.3). 120 μ m was etched using the small tube to confine the etching area. 30% Potassium hydroxide (KOH) solution was used for this wet etching process for 7hours @52⁰C temperature. Then the etching continues with the area defined by the larger tube. After 7.5 hours the area etched by the small tube opened and the KOH solution drained into the beaker. The remaining wafer had the thickness of 120 μ m.

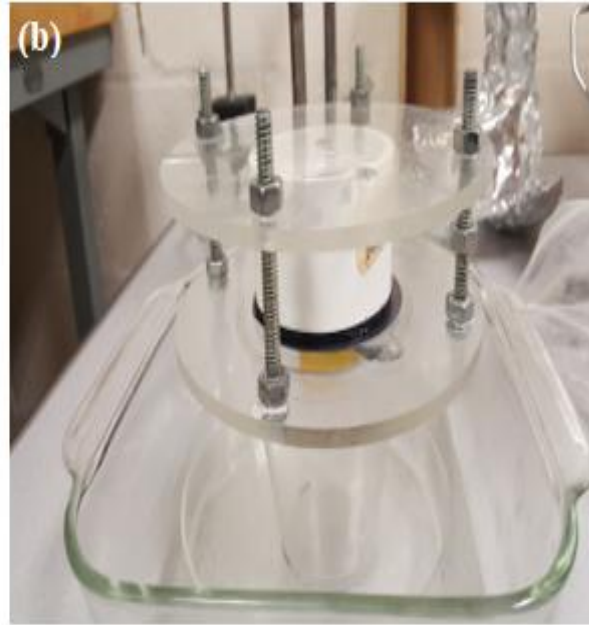
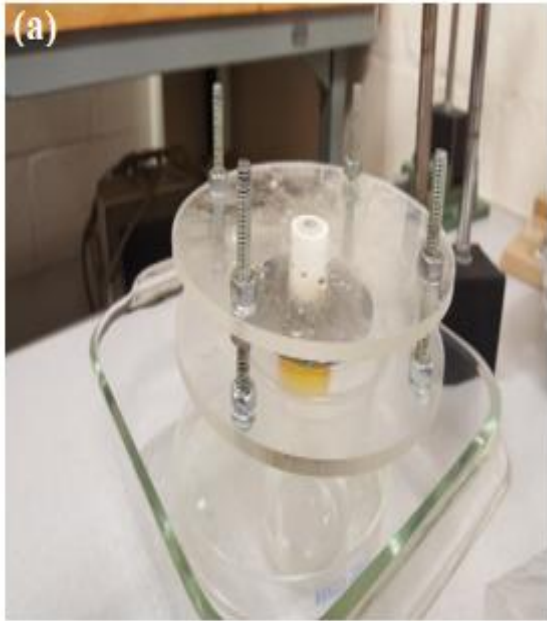


Figure 8.2. (a) Photograph of the etching set up using small tube (b) Photograph of the etching set up using large tube



Figure 8.3. Optical image of the Silicon wafer after removing 120 μm using small tube to define the etched area.

8.2.3 Gold Deposition on the Etched Silicon Wafer

After making the wafer thinner 20nm thick gold was sputtered on the smooth side of the etched Si wafer. The nano gaps between the gold islands on the wafer create an ideal surface for enhancement. The SEM image of this SERS substrate is shown below (Figure 8.4).

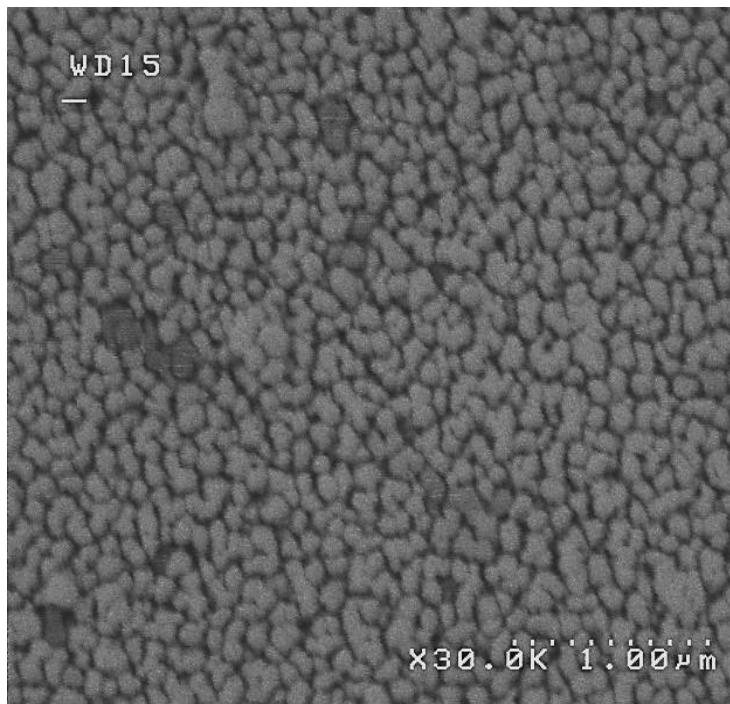


Figure 8.4 SEM image of the sputtered Au on smooth side of the silicon wafer under 30,000 X magnification.

8.3 Results

1mM R6G solution was used as a specimen for the in-vitro measurement. A single drop of R6G solution was placed on the gold nano-structure of the Si wafer and covered with cover slip to get a flat surface as well as to delay evaporation. The measurements were done immediately after adding the drop. A Raman spectrum obtained by this process using the 50X microscope objective (NA= 0.55) is shown below (Figure 8.5).

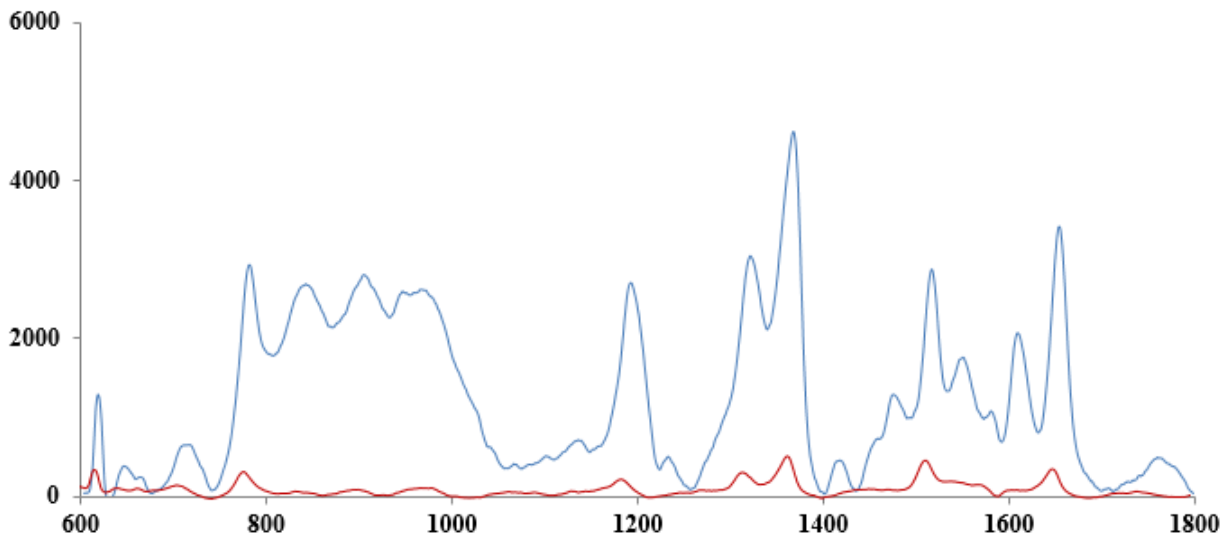


Figure 8.5 Raman spectrum of the 1mM R6G solution on the SERS substrate and on the smooth side of the bare Si wafer was obtained. The blue curve is the spectrum from 1mM R6G solution on the gold SERS substrate, and the red curve is the spectrum from 1mM R6G solution on the smooth side of the bare Si wafer.

The main peaks of the R6G solution at 610, 1310, 1360, 1647 cm^{-1} are prominent in this spectrum. The Raman spectrum from 1mM R6G solution on the smooth side of the bare Si wafer is also shown (Figure 8.7) as a reference. SERS signals were obtained from 1nM to 1mM R6G concentrations. Over a factor of 10^6 changes in concentration the Raman intensity changed by a factor of 195 (Figure 8.8). All the data are reproducible to about $\pm 10\%$.

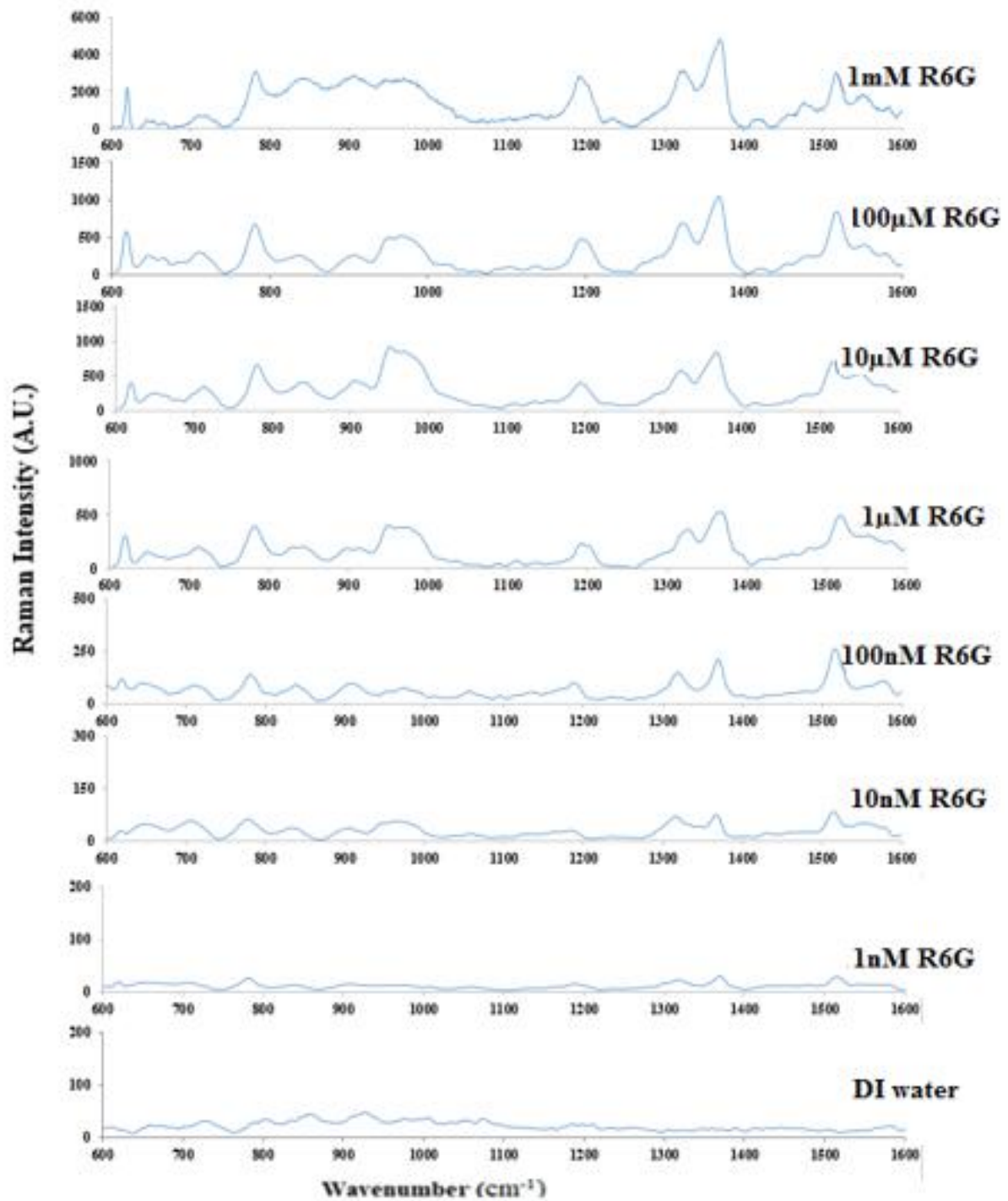


Figure 8.6 Raman signals of R6G solutions (using microscope objective of NA= 0.55) for viewing on gold on the smooth side of silicon wafer, as a function of the wave number. The concentration of R6G varied from 1nM to 1mM in steps of 10.

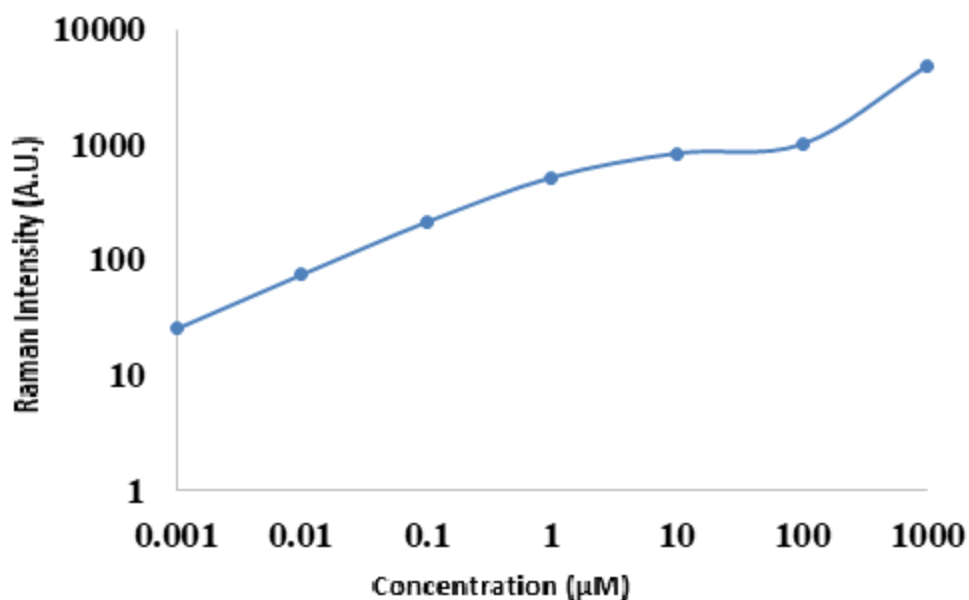


Figure 8.7 Raman signals (using 50x microscope objective) for viewing on gold as a function of the concentration of R6G solutions.

The SERS substrate was epoxied to an end of an optical fiber connected to a GRIN lens. The Si wafer was etched away after the epoxy had completely hardened. The process was the same as described previously (Chapter 5, section 5.3, Figure 5.7). After preparing the probe with Si wafer based SERS substrate it was attached at the end of an articulated arm. The Raman signal (Figure 8.8) from a gelatin block prepared with 1mM R6G solution was obtained in order to check the performance of this whole the set up.

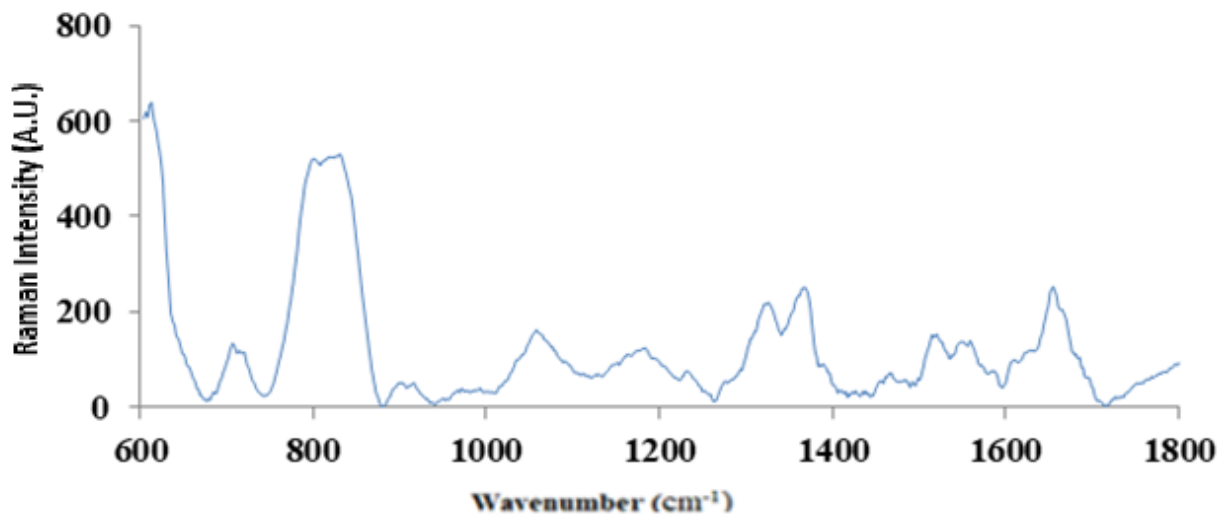


Figure 8.8 Raman signal of 1mM R6G in gelatin using optical fiber probe developed by Au coated silicon wafer.

8.4 Conclusion

This Chapter reports the development of a new, low cost SERS substrate by thinning the Si wafer and sputtering Au on it. In addition, a needle probe is developed with an optical fiber and this substrate.

CHAPTER 9: SUMMARY AND RECOMMENDATIONS FOR FUTURE WORK

9.1 Summary of Results

Three new Surface Enhanced Raman Scattering (SERS) substrates were developed by using (1) aluminum foil with gold, (2) carbon nanotube laden aluminum foil with gold, and (3) silicon wafer with gold. Of these three SERS substrates, the carbon nanotube laden aluminum foil with gold had the maximum enhancement (Table 9.1).

Table 9.1 Comparison of 3 newly developed SERS substrates

Type of the SERS substrate	Raman Intensity for 1mM R6G solution on the SERS substrate
Aluminum foil with gold	11693
Carbon nanotube laden aluminum foil with gold	21500
Silicon wafer with gold	4850

A new method was developed to fabricate rough metal nano structures at the end of an optical fiber in a needle. The needle probe was connected to a Raman spectrometer through an articulated arm and inserted into Gelatin blocks prepared with different concentrations of Rhodamine6G solutions. This single fiber SERS probe produced a strong signal, comparable to the same NA microscope objective in a conventional *in vitro* set up. It was many times greater than the signal produced by multiple fiber systems. Nano particles are not needed to be inserted and/or removed at the specimen site as in previously designed probes using multiple fibers. ^{[45, 47,}

61]

This minimally invasive system successfully distinguished cancerous colon tissues from the healthy colon of freshly sacrificed mice. This system not only reduces the post procedural risk of biopsy for cancer detection but reduces the cancer detection time, and permits a single insertion to examine multiple sites. Probes designed with Al foil and Au based SERS substrates were used for this purpose. The probe sensitivity was optimized with a SERS substrate using carbon nanotube laden Al foil covered with Au.

9.2 Recommendations for future work

The surface enhancement of Raman spectra is a complex phenomenon strongly dependent on the morphology of the rough metallic surface. Accordingly, we will evaluate Raman enhancement for sputtered and evaporated gold films for (1) average thickness, (2) deposition angle, (3) proximity to chamber sidewalls or other structures, and (4) material and morphology of substrate. Complex substrates, e.g., arrays of carbon nanotubes, are of particular interest.

Since the Raman signal is proportional to the square of the numerical aperture of the fiber, we will construct probes with higher NA optical fibers than are available in the GRIN lens/fiber assembly.

Probes with curved and angled tips can be developed so that the probe can look to the side as well as to the front, and we will evaluate thinner, less invasive, but more fragile needles.

Lighter, more easily manipulated arms with higher optical transmission and more sections for greater flexibility will be developed. The goal is for the arm to be as convenient for a technician to use as the arm which drives a dentist's drill. Hollow optical fibers will be evaluated as more flexible replacements for the articulate arm.

Applications other than cancer detection, e.g., cartilage and arthritis [91- 98] will also be evaluated.

9.3 Final remarks

The minimally invasive probe developed here brings Raman spectroscopy closer to a clinical environment, permitting cancer diagnosis.

REFERENCES

- [1] <http://drsnprasadmysoreindia.blogspot.com/2012/02/commemorating-historical-achievement.html>
- [2] C. V. Raman and K. S. Krishnan, "A new type of secondary radiation", *Nature*, 121(3048), 501-502 (1928).
- [3] https://en.wikipedia.org/wiki/Raman_scattering
- [4] N. P. Picczonka and R. F. Aroca, "Single molecule analysis by surfaced enhanced Raman scattering", *Chemical Society Reviews*, 37(5), 946–954 (2008).
- [5] H. Schulz and M. Baranska, "Identification and quantification of valuable plant substances by IR and Raman spectroscopy", *Vibrational Spectroscopy*, 43(1), 13–25 (2007).
- [6] D. A. Stuart, J. M. Yuen, N. Shah, O. Lyandres, C. R. Yonzon, M. R. Glucksberg et al., "In vivo glucose measurement by surface-enhanced Raman spectroscopy", *Analytical Chemistry*, 78(20), 7211–7215 (2006).
- [7] S. Keren, C. Zavaleta, Z. Cheng, A. de La Zerda, O. Gheysens, and S. Gambhir, "Noninvasive molecular imaging of small living subjects using Raman spectroscopy", *Proceedings of the National Academy of Science*, 105(15), 5844–5849 (2008).
- [8] C. L. Zavaleta, E. Garai, J. T. Liu, S. Sensarn, M. J. Mandella, D. Van de Sompel et al., "A Raman-based endoscopic strategy for multiplexed molecular imaging", *Proceedings of the National Academy of Science*, 110(25), E2288–E2297 (2013).
- [9] S. Nie and S. R. Emory, "Probing single molecules and single nanoparticles by surface-enhanced Raman scattering", *Science*, 275(5303), 1102–1106 (1997).
- [10] E. Le Ru and P. Etchegoin, "Principles of Surface-Enhanced Raman Spectroscopy: and related plasmonic effects", Elsevier (2008).
- [11] H.-C. Hou, *Nano Cost Nano Patterned Template for Surface Enhanced Raman Scattering (SERS) For IN-VITRO and IN-VIVO Applications* (Louisiana State University, 2016).
- [12] <http://bwtek.com/raman-theory-of-raman-scattering>
- [13] C. Kittel and D. F. Holcomb, "Introduction to solid state physics", *American Journal of Physics*, 35(6), 547-548 (1967).
- [14] <http://www.renishaw.com/en/why-we-use-raman-spectroscopy--25803>
- [15] <https://www.ukessays.com/essays/sciences/raman-spectroscopy.php>

[16] http://web.pdx.edu/~larosaa/Applied_Optics_464564/Projects_Optics/Raman_Spectroscopy/Raman_Spectroscopy_Basics_PRINCETON-INSTRUMENTS.pdf

[17] https://en.wikipedia.org/wiki/Surface-enhanced_Raman_spectroscopy

[18] J. A. Dieringer, A. D. McFarland, N. C. Shah, D. A. Stuart, A. V. Whitney, C. R. Yonzon, M. A. Young, X. Zhang and R. P. Van Duyne, "Introductory Lecture: Surface enhanced Raman spectroscopy: new materials, concepts, characterization tools, and applications", *Faraday Discussions*, 132, 9-26 (2006).

[19] E. C. L. Ru, E. Blackie, M. Meyer and P. G. Etchegoin, "Surface Enhanced Raman Scattering Enhancement Factors: A Comprehensive Study", *The Journal of Physical Chemistry C*, 111(37), 13794-13803 (2007).

[20] http://web.pdx.edu/~larosaa/Applied_Optics_464-564/Projects_Optics/Raman_Spectroscopy/Raman_Spectroscopy_Basics_PRINCETON-INSTRUMENTS.pdf

[21] G. C. Schatz, and R. P. Van Duyne, "Electromagnetic mechanism of surface-enhanced spectroscopy", *Handbook of vibrational spectroscopy* (2002).

[22] https://en.wikipedia.org/wiki/Surface-enhanced_Raman_spectroscopy.

[23] P. Kambhampati, C. M. Child, M. C. Foster, and A. Campion, "On the chemical mechanism of surface enhanced Raman scattering: experiment and theory", *The Journal of chemical physics*, 108(12), 5013-5026 (1998).

[24] T. W. Koo, S. Chan, L. Sun, X. Su, J. Zhang, and A. A. Berlin, "Specific chemical effects on surface-enhanced Raman spectroscopy for ultra-sensitive detection of biological molecules", *Applied spectroscopy*, 58(12), 1401-1407 (2004).

[25] H. Yamada, Y. Yamamoto, and N. Tani, "Surface-enhanced raman scattering (SERS) of adsorbed molecules on smooth surfaces of metals and a metal oxide", *Chemical Physics Letters*, 86(4), 397-400 (1982).

[26] M. J. Liew, S. Roy, and K. Scott, "Development of a non-toxic electrolyte for soft gold electrodeposition: an overview of work at University of Newcastle upon Tyne", *Green Chemistry* 5(4), 376-381 (2003).

[27] Von Ardenne M. Improvements in electron microscopes. GB 511204, convention date (Germany) 18 February 1937.

[28] https://en.wikipedia.org/wiki/Scanning_electron_microscope#cite_note-vonardenne-5

[29] https://serc.carleton.edu/research_education/geochemsheets/techniques/SEM.html

- [30] M. E. Wieser and T. B. Coplen, "Atomic weights of the elements 2009 (IUPAC Technical Report)", *Pure and Applied Chemistry*, 83(2), 359-396 (2010).
- [31] A. Seidell, W. F. Linke, A. W. Francis, and R. G. Bates, "Solubilities of inorganic and organic compounds: supplement to the third edition containing data published during the years 1939-1949 inclusive: a compilation of quantitative solubility data from the periodical literature", American Chemical Society (1952).
- [32] T. J. Bruno and P. D. Svoronos, *CRC handbook of basic tables for chemical analysis*: CRC press (2003).
- [33] J. Kim, "Clinical probe utilizing surface-enhanced Raman scattering (SERS) for *in-situ* molecular imaging applications", Ph.D. dissertation (Louisiana State University, 2015).
- [34] Hsuan-Chao Hou, Yaser Mohammadi Banadaki, Srismrita Basu, Subhodip Maulik, Shu-Wei Yang, Safura Sharifi, Martin Feldman. "Characterization of Sputtered Nano-Au Layer Deposition on Silicon Wafer", *International Journal of Advanced Research Trends in Engineering and Technology*, 3(12), 12 (2016).
- [35] Y. C. Yang, T. K. Huang, Y. L. Chen, J. Y. Mevellec, S. Lefrant, C.-Y. Lee and H.-T. Chiu, "Electrochemical growth of gold nanostructures for surface-enhanced Raman scattering", *The Journal of Physical Chemistry C*, 115(5), 1932-1939 (2011).
- [36] K. Kneipp, Y. wang, R. R Dasari, M. S, Feld, "Approach to single molecule detection using surface-enhanced resonance Raman scattering (SERRS): A study using Rhodamine 6G on colloidal silver", *Applied spectroscopy*, 49(6), 780-784 (1995).
- [37] M. Suzuki, Y. Niidome, N. Terasaki, K. Inoue, Y. Kuwahara, and S. Yamada, "Surface-enhanced nonresonance Raman scattering of rhodamine 6G molecules adsorbed on gold nanorod films", *Japanese journal of applied physics*, 43(4B), L554 (2004).
- [38] R. Z. Tan, A. Agarwal, N. Balasubramanian, D. L. Kwong, Y. Jiang, E. Widjaja, and M. Garland, "3D arrays of SERS substrate for ultrasensitive molecular detection" *Sensors and Actuators A: Physical*, 139(1), 36-41 (2007).
- [39] X. N. He, Y. Gao, M. Mahjouri-Samani, P. N. Black, J. Allen, M. Mitchell, W. Xiong, Y. S. Zhou, L. Jiang and Y. F. Lu, "Surface-enhanced Raman spectroscopy using gold-coated horizontally aligned carbon nanotubes", *Nanotechnology*, 23(20), 205702 (2012).
- [40] J. Rose, S. Pacelli, A. Haj, H. Dua, A. Hopkinson, L. White and F. Rose, "Gelatin-based materials in ocular tissue engineering", *Materials*, 7(4), 3106-3135 (2014).
- [41] J. Kim, D. Hah, T. Daniels-Race, and M. Feldman, "Clinical probe utilizing surface enhanced Raman scattering", *Journal of Vacuum Science Technology B, Nanotechnology and Microelectronics: Materials*, 32(6), 06FD02 (2014).

- [42] H. C. Hou, J. Kim, K. Kanakamedala, S. Basu, T. Daniels-Race, M. Feldman, "Nano cost nano patterned template for surface enhanced Raman Scattering", presented at the International Conference on Electron, Ion and Photon Beam Technology and Nanofabrication, San Diego, CA, 26–29 May 2015.
- [43] R. L. McCreery, M. Fleischmann, and P. Hendra, "Fiber optic probe for remote Raman spectrometry", *Analytical Chemistry*, 55(1), 146–148 (1983).
- [44] Y. Komachi, H. Sato, K. Aizawa, and H. Tashiro, "Micro-optical fiber probe for use in an intravascular Raman endoscope", *Applied Optics*, 44(22), 4722–4732 (2005).
- [45] M. Sharma, E. Marple, J. Reichenberg, and J. W. Tunnell, "Design and characterization of a novel multimodal fiber-optic probe and spectroscopy system for skin cancer applications", *Review of Scientific Instruments*, 85(2), 083101 (2014).
- [46] S. Basu, H. C. Hou, D. Biswas, S. Maulik, T. Daniels-Race, M. Lopez, M. Mathis, and M. Feldman, "A needle probe to detect surface enhanced Raman scattering (SERS) within solid specimen" *Review of Scientific Instruments*, 88 (2), 023107 (2017)
- [47] J. T. Motz, M. Hunter, L. H. Galindo, J. A. Gardecki, J. R. Kramer, R. R. Dasari, and M. S. Feld, "Optical fiber probe for biomedical Raman spectroscopy", *Applied Optics*, 43(3), 542-554 (2004).
- [48] Y. Komachi, , H. Sato, K. Aizawa, and H. Tashiro, "Micro-optical fiber probe for use in an intravascular Raman endoscope", *Applied Optics*, 44(22), 4722-4732 (2005).
- [49] L. F. Santos, R. Wolthuis, S. Koljenović, R. M. Almeida, and G. J. Puppels, "Fiber-optic probes for in vivo Raman spectroscopy in the high-wavenumber region", *Analytical chemistry*, 77(20), 6747-6752 (2005).
- [50] P. Baptista, E. Pereira, P. Eaton, G. Doria, A. Miranda, I. Gomes, P. Quaresma, and R. Franco, "Gold nanoparticles for the development of clinical diagnosis methods", *Analytical and bioanalytical chemistry*, 391(3), 943-950 (2008).
- [51] F. Colas, D. Barchiesi, S. Kessentini, T. Toury, and M. Lamy de la Chapelle, "Comparison of adhesion layers of gold on silicate glasses for SERS detection", *Journal of Optics*, 17(11), 114010 (2015).
- [52] D. L. Stokes, Z. Chi, and T. Vo-Dinh, "Surface-enhanced-Raman-scattering-inducing nanoprobe for spectrochemical analysis", *Applied spectroscopy*, 58(3), 292-298 (2004).
- [53] D. Li, Y. Wang, and Y. Xia, "Electrospinning nanofibers as uniaxially aligned arrays and layer-by-layer stacked films", *Advanced Materials*, 16(4), 361-366 (2004).

- [54] S. Marx, M. V. Jose, J. D. Andersen, and A. J. Russell, "Electrospun gold nanofiber electrodes for biosensors", *Biosensors and Bioelectronics*, 26(6), 2981-2986, (2011).
- [55] S. Basu, H. C. Hou, D. Biswas, T. Daniels-Race, M. Lopez, M. Mathis, and M. Feldman, "A Single Fiber Surface Enhanced Raman Scattering (SERS) Probe", *Journal of Vacuum Science B, Nanotechnology and Microelectronics: Materials, Processing, Measurement, and Phenomena*, 35(6), 06GF01 (2017).
- [56] S. Winawer, R. Fletcher, D. Rex, J. Bond, R. Burt, J. Ferrucci, T. Ganiats, T. Levin, S. Woolf, D. Johnson, L. Kirk, S. Litin, C. Simmong, "Colorectal cancer screening and surveillance: clinical guidelines and rationale—update based on new evidence", *Gastroenterology*, 124(2), 544-560 (2003).
- [57] R. W. Burt, "Colon cancer screening", *Gastroenterology*, 119(3), 837-853 (2000).
- [58] J. C. Presti, G. J. O'dowd, M. C. Miller, R. Mattu, and R. W. Veltri, "Extended peripheral zone biopsy schemes increase cancer detection rates and minimize variance in prostate specific antigen and age related cancer rates: results of a community multi-practice study", *The Journal of urology*, 169(1), 125-129 (2003).
- [59] J. W. Fowler, S. A. Bigler, D. Miles, and D. A. Yalkut, "Predictors of first repeat biopsy cancer detection with suspected local stage prostate cancer" *The Journal of urology*, 163(3), 813-818 (2000).
- [60] F. Frauscher, A. Klauser, H. Volgger, E. J. Halpern, L. Pallwein, H. Steiner, A. Schuster, W. Horninger, H. Rogatsch, and G. Bartsch, "Comparison of contrast enhanced color Doppler targeted biopsy with conventional systematic biopsy: impact on prostate cancer detection", *The Journal of urology*, 167(4), 1648-1652 (2002).
- [61] S. Schnittger, C. Schoch, M. Dugas, W. Kern, P. Staib, C. Wuchter, H. Löffler, C. M. Sauerland, H. Serve, T. Buchner, T. Haferlach, W. Hiddemann, "Analysis of FLT3 length mutations in 1003 patients with acute myeloid leukemia: correlation to cytogenetics, FAB subtype, and prognosis in the AMLCG study and usefulness as a marker for the detection of minimal residual disease", *Blood*, 100(1), 59-66 (2002).
- [62] R. Clements, O. U. Aideyan, G. J. Griffiths, and W. B. Peeling, "Side effects and patient acceptability of transrectal biopsy of the prostate", *Clinical radiology*, 47(2), 125-126 (1993).
- [63] F. J. García-Vidal and J. B. Pendry, "Collective theory for surface enhanced Raman scattering", *Physical Review Letters*, 77(6), 1163 (1996).
- [64] X. Li, G. Chen, L. Yang, Z. Jin, and J. Liu, "Multifunctional Au-Coated TiO₂ Nanotube Arrays as Recyclable SERS Substrates for Multifold Organic Pollutants Detection" *Advanced Functional Materials*, 20(17), 2815-2824 (2010).

- [65] Z. Niu, and Y. Fang, Surface-enhanced Raman scattering of single-walled carbon nanotubes on silver-coated and gold-coated filter paper", *Journal of colloid and interface science*, 303(1), 224-228 (2006).
- [66] C. J. L. Constantino, T. Lemma, P. A. Antunes, and R. Aroca, "Single-molecule detection using surface-enhanced resonance Raman scattering and Langmuir– Blodgett monolayers." *Analytical Chemistry*, 73(15), 3674-3678 (2001).
- [67] S. Shanmukh, L. Jones, J. Driskell, Y. Zhao, R. Dluhy, and R. A. Tripp, "Rapid and sensitive detection of respiratory virus molecular signatures using a silver nanorod array SERS substrate," *Nano Letters*, 6(11) 2630-2636 (2006).
- [68] W. J.Cho, Y. Kim, and J. K. Kim, "Ultrahigh-density array of silver nanoclusters for SERS substrate with high sensitivity and excellent reproducibility", *ACS nano*, 6(1), 249-255 (2011).
- [69] A. Alexiadis, and S. Kassinos, "Molecular simulation of water in carbon nanotubes", *Chemical Reviews*, 108(12), 5014-5034, (2008).
- [70] T. A. Pascal, W. A. Goddard, and Y. Jung, "Entropy and the driving force for the filling of carbon nanotubes with water", *Proceedings of the National Academy of Sciences* 108(29), 11794-11798 (2011).
- [71] P. C. Ma, N. A. Siddiqui, G. Marom, and J. K. Kim, "Dispersion and functionalization of carbon nanotubes for polymer-based nanocomposites: a review", *Composites Part A: Applied Science and Manufacturing*, 41(10), 1345-1367 (2010).
- [72] C. C. Teng, C. C. M. Ma, Y. W. Huang, S. M. Yuen, C. C. Weng, C. Ho Chen, and S. F. Su, "Effect of MWCNT content on rheological and dynamic mechanical properties of multiwalled carbon nanotube/polypropylene composites", *Composites Part A: Applied Science and Manufacturing*, 39(12), 1869-1875 (2008).
- [73] S. L. Jiang, Y. Yu, J. J. Xie, L. P. Wang, Y. K. Zeng, M. Fu, and T. Li, "Positive temperature coefficient properties of multiwall carbon nanotubes/poly (vinylidene fluoride) nanocomposites", *Journal of applied polymer science*, 116(2), 838-842 (2010).
- [74] M. S. Dresselhaus, G. Dresselhaus, P. C. Eklund, and A. M. Rao, "In The Physics of Fullerene-Based and Fullerene-Related Materials; Anderoni, W., Ed.", Springer: Netherlands, 331-379 (2000).
- [75] B. I. Yakobson, and P. Avouris, "Mechanical properties of carbon nanotubes", In *Carbon nanotubes*, Springer Berlin Heidelberg, 287-327 (2001).
- [76] https://en.wikipedia.org/wiki/Carbon_nanotube
- [77] Private communication with Dr. Theda Daniels-Race, Louisiana State University, (11/15/2016).

- [78] S. Maulik, S. Basu, H. C. Hou, and T. Daniels-Race, "Voltage-Controlled Deposition of Carbon Nanotubes onto a Conducting Substrate without a Catalyst", *Advanced Science, Engineering and Medicine*, 10, 1-4 (2018).
- [79] A. Sarkar, and T. Daniels-Race, "Electrophoretic deposition of carbon nanotubes on 3-amino-propyl-triethoxysilane (APTES) surface functionalized silicon substrates", *Nanomaterials*, 3(2), 272-288 (2013).
- [80] A. Sarkar, and D. Hah, "Electrophoretic deposition of carbon nanotubes on silicon substrates", *Journal of electronic materials*, 1-9 (2012).
- [81] K. Kanakamedala, J. DeSoto, A. Sarkar, and T. Daniels Race, "Study of electrospray assisted electrophoretic deposition of carbon nanotubes on insulator substrates", *Electronic Materials Letters*, 11(6), 949-956 (2015).
- [82] A. Sarkar, "Electrophoretic deposition of carbon nanotubes on silicon substrates", Ph.D. dissertation (Louisiana State University, 2013).
- [83] K. C. Kanakamedala, "Hybrid Electronic Materials: Characterization and Thin-film Deposition", Ph.D. dissertation (Louisiana State University, 2015).
- [84] M. L. Terranova, V. Sessa, and M. Rossi, "The world of carbon nanotubes: an overview of CVD growth methodologies", *Chemical Vapor Deposition*, 12(6), 315-325 (2006).
- [85] J. N. Crosby, and R. S. Hanley, U.S. Patent 4, 250, 210 (1981).
- [86] A. Szabó, C. Perri, A. Csato, G. Giordano, D. Vuono, and J. B. Nagy, "Synthesis methods of carbon nanotubes and related materials", *Materials* 3(5), 3092-3140 (2010).
- [87] M. Danen, R. D. De fouw, B. Hamers, P. G. A. Janssen, K. Schouteden, and M. A. J. Veld, Eindhoven University of Technology 27 (2003).
- [88] S. Maulik, S. Basu, and T. Daniels-Race, *Bulletin of the American Physical Society* 61 (2016).
- [89] S. Basu, S. Maulik, H. C. Hou, T. Daniels-Race and M. Feldman, "Surface Enhanced Raman Spectroscopic Substrate Utilizing Gold Nanoparticles on Carbon Nanotubes", *Journal of Applied Physics*, 122(12) (2017).
- [90] J. A. Dieringer, K. L. Wustholz, D. J. Masiello, J. P. Camden, S. L. Kleinman, G. C. Schatz, and R. P. Van Duyne, "Surface-enhanced Raman excitation spectroscopy of a single rhodamine 6G molecule", *Journal of the American Chemical Society* 131(2), 849-854 (2008).
- [91] P. T. Paradowski, "Osteoarthritis of the knee: Assessing the disease", *Health Care: Current Reviews*, 2(2), 1-2 (2014).

- [92] A. Guermazi, F. W. Roemer, D. Burstein and D. Hayashi, "Why radiography should no longer be considered a surrogate outcome measure for longitudinal assessment of cartilage in knee osteoarthritis", *Arthritis Research & Therapy*, 13(6), 247 (2011).
- [93] I. Haq, E. Murphy and J. Dacre, "Osteoarthritis", *Postgraduate Medical Journal*, 79(933), 377-383 (2003).
- [94] Y. Zhang and J. M. Jordan, "Epidemiology of osteoarthritis", *Clinics in Geriatric Medicine*, 26(3), 355-369 (2010).
- [95] Y. Takahashi, N. Sugano, M. Takao, T. Sakai, T. Nishii and G. Pezzotti, "Raman spectroscopy investigation of load-assisted microstructural alterations in human knee cartilage: Preliminary study into diagnostic potential for osteoarthritis", *Journal of the Mechanical Behavior of Biomedical Materials*, 31, 77-85 (2014).
- [96] A. Carden, R. M. Rajachar, M. D. Morris and D. H. Kohn, "Ultrastructural changes accompanying the mechanical deformation of bone tissue: a Raman imaging study", *Calcif Tissue International*, 72(2), 166-175 (2003).
- [97] J. F. de la Mora, "The fluid dynamics of Taylor cones", *Annual Review of Fluid Mechanics*, 39, 217-243 (2007).
- [98] Z. Chen, Z. Dai, N. Chen, S. Liu, F. Pang, B. Lu, and T. Wang, "Gold nanoparticles-modified tapered fiber nanoprobe for remote SERS detection", *IEEE Photonics Technology Letters*, 26(8), 777-780 (2014).

APPENDIX A: PERMISSION TO REPRINT FROM REVIEW OF SCIENTIFIC INSTRUMENTS

From: Srismrita Basu [<mailto:sbasu9@lsu.edu>]
Sent: Monday, October 9, 2017 1:17 PM
To: AIPRights Permissions <Rights@aip.org>
Subject: Asking for a permission to reuse my paper in thesis

Dear Sir,

I published a paper named "A needle probe to detect surface enhanced Raman scattering (SERS) within solid specimen" in Review of Scientific instruments on February 2017. I want to use this paper with some additions in my thesis. I am the first and the major author of the paper. Can you please let me know how can I do this/ can get the permission for it? I am attaching the paper for your ease.

Thanking you.

Best regards,
Srismrita Basu
Graduate Research Assistant
Louisiana State University

Sent: Monday, October 9, 2017 12:35:11 PM
To: Srismrita Basu
Subject: RE: Asking for a permission to reuse my paper in thesis

Dear Dr. Basu:

You are permitted to include your published article in your thesis, provided you also include a credit line referencing the original publication.

Our preferred format is (please fill in the citation information):

"Reproduced from [FULL CITATION], with the permission of AIP Publishing."

Please let us know if you have any questions.

Sincerely,
Susann Brailey
Manager, Rights & Permissions

AIP Publishing
1305 Walt Whitman Road | Suite 300 | Melville NY 11747-4300 | USA
t +1.516.576.2268
rights@aip.org | publishing.aip.org
Follow us: [Facebook](#) | [Twitter](#) | [LinkedIn](#)

Dear Susann,

Thank you so much. I have two more questions.

(1) I want to add some more lines and figures along with the published paper in RSI in a single chapter in my thesis. So, in that case should I write it as "Reproduced with changes from [FULL CITATION], with the permission of AIP Publishing." after the chapter heading?

(2) Another thing is do I need to add this thing at the end of each image as well?

Thanking you.

Best regards,

Srismrita Basu

Dear Dr. Basu:

The changes to the credit line are okay.

If you are using the images separate from the article itself, then you should include the credit lines in the captions with each use.

Thanks very much.

Sincerely,

Susann Brailey

Manager, Rights & Permissions

AIP Publishing

1305 Walt Whitman Road | Suite 300 | Melville NY 11747-4300 | USA

t +1.516.576.2268

rights@aip.org | publishing.aip.org

Follow us: [Facebook](#) | [Twitter](#) | [LinkedIn](#)




AIPRights Permissions <Rights@aip.org>

Tue 10/10, 12:14 PM

Srismrita Basu 



Reply all | 

Dear Dr. Basu:

We don't have a formal letter. Usually, the email is sufficient.

Thanks very much.

Sincerely,

Susann Brailey

Susann Brailey

Manager, Rights & Permissions

AIP Publishing

1305 Walt Whitman Road | Suite 300 | Melville NY 11747-4300 | USA

t +1.516.576.2268

rights@aip.org | [\[publishing.aip.org\]publishing.aip.org](http://publishing.aip.org)

Follow us: [Facebook](#) | [Twitter](#) | [LinkedIn](#)

**APPENDIX B: PERMISSION TO REPRINT FROM JOURNAL OF VACUUM SCIENCE
& TECHNOLOGY B, NANOTECHNOLOGY AND MICROELECTRONICS:
MATERIALS, PROCESSING, MEASUREMENT, AND PHENOMENA**

Asking for permission

Srismrita Basu

Fri 10/20/2017 12:36 PM

Sent Items

to:rights@aip.org <rights@aip.org>;

1 attachment (1 MB)

JVST B 2017.pdf

Dear Sir/Madam,

I published a paper named "Single fiber surface enhanced Raman scattering probe" in Journal of Vacuum Science & Technology B, Nanotechnology and Microelectronics: Materials, Processing, Measurement, and Phenomena 35, 06GF01 (2017); doi: 10.1116/1.4990697".

I want to use this paper with some additions in my thesis. I am the first and the major author of the paper. Can you please let me know how can I do this/ can get the permission for it? I am attaching the paper for your ease.

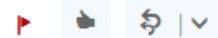
Thanking you.

Best regards,
Srismrita Basu
Graduate Research Assistant
Louisiana State University



AIPRights Permissions <rights@aip.org>

Mon 10/23, 8:47 AM



Dear Dr. Basu:

You are permitted to include your published article in your thesis, provided you also include a credit line referencing the original publication.

Our preferred format is (please fill in the citation information):

"Reproduced from [FULL CITATION], with the permission of AIP Publishing."

Please let us know if you have any questions.

Sincerely,

Susann Brailey

Manager, Rights & Permissions

AIP Publishing

[1305 Walt Whitman Road | Suite 300 | Melville NY 11747-4300 | USA](#)

t +1.516.576.2268

rights@aip.org | publishing.aip.org

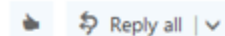
Follow us: [Facebook](#) | [Twitter](#) | [LinkedIn](#)



Srismrita Basu

Mon 10/23, 9:08 AM

AIPRights Permissions <rights@aip.org> ✉



Dear Madam,

Thank you so much. As I will add the paper with some changes, I believe I have to add the credit line as

"Reproduced with changes from [full citation] with the permission from AIP Publishing."

Please let me know if I am correct or not?

Best regards,

Srismrita Basu

Get [Outlook for Android](#)

...

Dear Dr. Basu:

The changes to the credit line are okay.

If you are using the images separate from the article itself, then you should include the credit lines in the captions with each use.

Thanks very much.

Sincerely,

Susann Brailey

Manager, Rights & Permissions

AIP Publishing

[1305 Walt Whitman Road | Suite 300 | Melville NY 11747-4300 | USA](#)

t +1.516.576.2268

rights@aip.org | [\[publishing.aip.org\]](http://publishing.aip.org)publishing.aip.org

Follow us: [Facebook](#) | [Twitter](#) | [LinkedIn](#)

APPENDIX C: PERMISSION TO REPRINT FROM JOURNAL OF APPLIED PHYSICS



Srismrita Basu

Fri 11/3, 11:30 AM

rights@aip.org <Rights@aip.org> ↕



Reply all | ▾

Dear Sir/Madam,

My name is Srismrita Basu, the first and the corresponding author of the paper named "Surface Enhanced Raman Spectroscopic Substrate Utilizing Gold Nanoparticles on Carbon Nanotubes". Manuscript #JR17-4736R1. It is going to be published In Journal of Applied Physics on 14th November. But, already accepted and manuscript checking is done as well.

I want to use this paper for my thesis. So, please let me know what should I do for getting the permission. Should I wait for the publication date? Or I can get the permission now.

Thanking you.

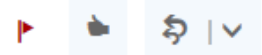
Best regards,
Srismrita Basu
Louisiana State University

About getting the permission



AIPRights Permissions <Rights@aip.org>

Today, 10:23 AM



Dear Dr. Basu:

You are permitted to include your published article in your thesis, provided you also include a credit line referencing the original publication. If you know the citation information for the article, please use the following credit line:

Our preferred format is (please fill in the citation information):

“Reproduced from [FULL CITATION], with the permission of AIP Publishing.”

If you do not yet know the citation information, please credit the work as follows:

“Accepted for publication in the Journal of Applied Physic. Once published, it will be found at (URL/link to the entry page of the journal).”

Please let us know if you have any questions.

Sincerely,
Susann Brailey
Manager, Rights & Permissions

AIP Publishing
[1305 Walt Whitman Road | Suite 300 | Melville NY 11747-4300 | USA](#)
t +1.516.576.2268
rights@aip.org | publishing.aip.org
Follow us: [Facebook](#) | [Twitter](#) | [LinkedIn](#)



VITA

Srismrita Basu was born to Debisree Bose and Srikumar Bose, in Baidyabati, West Bengal, India in 1986. She did her schooling from Serampore Girls' High School, India. She received her Bachelor degree (B.Sc, Honors) in Physics from University of Calcutta, India, in May 2006. In 2008 she finished her first master degree (M.Sc) in Electronic Science from University of Calcutta, and in 2010 she earned her second master degree (M.Tech) in Electronics and Communication Engineering. She was working as an Assistant Professor from 2009 to 2013 in Greater Kolkata College of Engineering and Management, India in Electronics department. She joined Louisiana State University, Baton Rouge, USA to pursue her Ph.D. in fall 2013 under the mentorship of Dr. Martin Feldman. Her research interests lie in probe designing, biological specimen detection, cancer detection, characterization and fabrication techniques, Surface Enhanced Raman Spectroscopy, SERS substrates fabrication. Her research topic for Ph.D. is "Surface Enhanced Raman Scattering (SERS) Substrates and Probes".